

Recent advances in nanogenerators driven by flow-induced vibrations for harvesting energy



Mengwei Wu ^a, Chuanqing Zhu ^b, Xiangtao Liu ^a, Hao Wang ^b, Jicang Si ^b, Minyi Xu ^{b,*}, Jianchun Mi ^{a,**}

^a College of Engineering, Peking University, Beijing 100871, China

^b Marine Engineering College, Dalian Maritime University, Dalian 116026, China

ARTICLE INFO

Article history:

Received 14 December 2023

Received in revised form

3 February 2024

Accepted 9 February 2024

Available online 12 February 2024

Keywords:

Flow-induced vibration

Fluid-structure interaction

Piezoelectric nanogenerator

Triboelectric nanogenerator

Energy harvesting

ABSTRACT

In recent years, remarkable strides have been achieved in the advancement of nanogenerators harnessing fluid-induced vibrations. This article comprehensively undertakes a methodical exploration of the latest advancements in the nanogenerator research centered around fluid-induced vibrations. To commence, the foundational principles of piezoelectric generation, contact electrification and fluid-induced vibration are elucidated, laying the groundwork for subsequent discourse. Following this, the article systematically categorizes manifold applications of piezoelectric nanogenerators (PENGs) and triboelectric nanogenerators (TENGs) within the realm of fluid-induced vibrations. This categorization offers insights into the diverse scenarios where these nanogenerators exhibit efficacy, further enriching the understanding of their potential. The theme of categorization extends the understanding of PENG and TENG applications within fluid-induced vibrations, augmenting the reader's grasp of their versatility and functional mechanisms. Subsequently, a comprehensive comparison of PENG and TENG is carried out to clarify the current challenges and provide suggestions for future development. Notably, the article highlights the growing significance of these technologies in fostering sustainable energy solutions. Its comprehensive analysis and systematic classification serve as a valuable reference for researchers and practitioners alike, propelling the field towards innovative applications and breakthroughs.

© 2024 Elsevier Ltd. All rights reserved.

1. Introduction

In the present era of digitization and mobility, the demand for miniature electronic devices is incessantly increasing [1–3]. From smartwatches to health monitoring devices, and from environmental sensing sensors to Internet of Things (IoT) systems, these devices are playing progressively crucial roles in people's everyday existence [4–6]. Nonetheless, the challenge of independent power supply for these diminutive devices persists as a notable concern. While conventional batteries partially fulfill energy demands, the escalating functionalities of devices and the consistent diminution in size are presenting progressively stringent limitations on energy density and continuous power delivery capabilities [7–10]. Frequently recharging, limited battery lifespan, and the perpetual

reliance on large-sized batteries have triggered a desire among people for a more sustainable and efficient energy supply [11–13]. To overcome these limitations, energy harvesting technology has been paid significant attention as an innovative and viable solution. Energy harvesting technology aims to capture minuscule forms of energy from the environment, such as wind energy [14–17], vibration energy [18–22], water flow energy [23–25], and convert it into electrical energy useable for power supply. In this realm, nanogenerator technology has received widespread interest due to its capacity to convert mechanical energy into electricity at the microscale [26–30]. By harnessing the unique properties of materials at the nanoscale, these technologies can effectively convert minuscule mechanical changes into voltage and current. Within the scope of nanogenerator technology, piezoelectric and triboelectric effects are two commonly employed mechanisms. The piezoelectric effect involves the generation of charge separation within a material when subjected to mechanical stress or pressure, leading to the creation of a potential difference [31–36]. Conversely, the triboelectric effect involves the separation of charges through friction between two dissimilar materials [37–41]. These two effects create

* Corresponding author.

** Corresponding author.

E-mail addresses: xuminyi@dlnu.edu.cn, minyixu@qq.com (M. Xu), jmi@pku.edu.cn (J. Mi).

intriguing opportunities for energy harvesting in nanogenerator devices.

Further, although modern battery technology, such as lithium-ion batteries, has made significant progress in offering relatively high energy density, PENG and TENG technologies, by contrast, convert ambient energies (such as mechanical and electrostatic energy) into electrical energy, providing a theoretically indefinite power supply. This showcases potential advantages in long-term deployment and sustainability. Second, from a sustainability perspective, the use of batteries involves the extraction, processing, and ultimate disposal of materials, which may have adverse environmental impacts, particularly in the case of batteries containing harmful heavy metals. In contrast, PENG and TENG technologies utilize existing environmental energies, such as human movement and vibrations. The development and application of these technologies reduce reliance on harmful materials, thus exhibiting significant advantages in environmental sustainability. Last, regarding lifespan, the usage life of batteries is limited by the number of charge-discharge cycles, meaning they require replacement after long-term use. PENG and TENG technologies, due to their operating principles, theoretically offer longer lifespans, especially in low-power sensor applications. In summary, while PENG and TENG technologies currently face challenges in energy output and stability, necessitating further research and development, their potential advantages in energy density, sustainability, and lifespan indeed constitute significant motivations for exploring alternatives to traditional battery solutions. We believe that with advancements in material science and nanotechnology, these technologies could provide more sustainable and long-term energy solutions for applications such as small sensors.

In recent years, the fluid-induced vibration has gained significant attention as a prominent mechanical energy source, prompting extensive research endeavors [42–46]. The fluid-induced vibration refers to mechanical oscillations generated by the flow of fluids, encompassing phenomena such as gentle breezes, water surges, and even air disturbances caused by human movement [47–52]. Within the realm of natural occurrences, numerous phenomena of fluid-induced vibration can be observed. The rustling of leaves in a gentle breeze, the motion of water through narrow passages, and the aerodynamic effects arising from human locomotion all exemplify those cases of fluid-induced vibration. Despite their seemingly minor motions in nature, these vibrations contain substantial mechanical energy, perhaps being a potential wellspring of energy. The concept of harnessing mechanical energy from fluid-induced vibrations is not new; however, recent technological advancements and engineering innovations have rendered this concept more realistic and viable. For instance, in the domain of architecture, researchers now incorporate fluid-induced vibration into wind energy generation devices [53–55]. By installing specially designed apparatuses on building facades or rooftops, fluid-induced vibrations can be captured under gentle winds, subsequently transforming them into electrical power. This technology not only furnishes renewable energy to buildings but also reduces reliance on conventional energy sources. Another crucial application area pertains to ocean energy harvesting systems [56–62]. Oceans harbor abundant kinetic energy within their currents, which can be harnessed by the fluid-induced vibration technology through deploying vibration devices underwater. These devices can be tailored according to the velocity and direction of ocean currents, thereby maximizing mechanical energy extraction. This offers a fresh avenue for sustainable exploitation of oceanic energy, potentially yielding positive impacts on energy supply.

In summary, the fluid-induced vibration, as a notable mechanical energy source, holds significance within the context of energy transition and sustainable development. Through ongoing research and innovation, we intend to harness fluid-induced vibration

technology to its fullest potential, providing clean and renewable energy solutions across diverse domains. This pursuit aligns with the dual objectives of technological advancement and environmental preservation. In this context, the integration of piezoelectric and triboelectric nanogenerator technologies with the phenomenon of fluid-induced vibrations has opened up new research avenues towards achieving self-sustained power supply for microdevices. The innovation of this approach lies in utilizing fluid-induced vibration as a mechanical energy source and converting it into electrical energy through piezoelectric and triboelectric effects, thereby offering a stable and sustainable energy source for microdevices [63–70]. What sets this approach apart is that it not only captures energy from the environment but also continuously generates energy during the normal operation of the device, requiring no additional intervention or energy input.

The far-reaching potential of nanogenerator technology, harnessed through the exploitation of fluid-induced vibration, extends far beyond the realm of self-powered microdevices, encompassing a diverse spectrum of domains [71–80]. The ingenious application of this technology holds particular promise in the realm of environmental monitoring, wherein sensors stand to derive their power from the very fluid motions that pervade the natural world. This visionary approach paves the way for unceasing data collection, addressing a critical need in today's data-driven society. Moreover, the ramifications of this technology ripple into the realm of sustainable energy solutions for remote and resource-scarce regions [81–83]. Inhabitants of areas bereft of stable electrical grids stand to benefit from the ingenuity embodied in these nanogenerators. These technologies can not only offer independent power to microdevices but also, to a certain extent, reduce reliance on conventional batteries and fossil fuels, thereby mitigating carbon emissions and environmental impacts [84–87]. In recent years, significant progress has been achieved in the field of nanogenerator technology by harnessing the phenomenon of fluid-induced vibration. By integrating the piezoelectric and triboelectric effects, researchers have effectively converted fluid-induced vibrations into electricity, providing a novel and sustainable energy source for microdevices [88–96]. Nevertheless, this field still confronts numerous challenges and opportunities. Improving material performance, enhancing device efficiency, addressing reliability and scalability in real-world applications, among other issues, demand further research and exploration. With the continuous development of nanotechnology and the growing demand for energy, piezoelectric and triboelectric nanogenerator technologies are poised to play a more significant role in the field of sustainable energy in the future.

This review comprehensively surveys recent significant advancements in the utilization of fluid-induced vibration phenomena in piezoelectric and triboelectric nanogenerator technologies. It systematically categorizes these developments according to different structural configurations (see Fig. 1). Through this review, we aim to offer researchers an opportunity to gain in-depth insights into the forefront dynamics of this field, foster the dissemination and development of nanogenerator technology in practical applications, and make a modest contribution to innovation in the energy sector. As time progresses, we anticipate that this field will continue to achieve further breakthroughs and accomplishments, contributing more possibilities to the sustainability of human development.

2. Theoretical background of nanogenerator and fluid-induced vibration

Piezoelectric nanogenerators (PENGs) and triboelectric nanogenerators (TENGs) convert mechanical energy into electrical

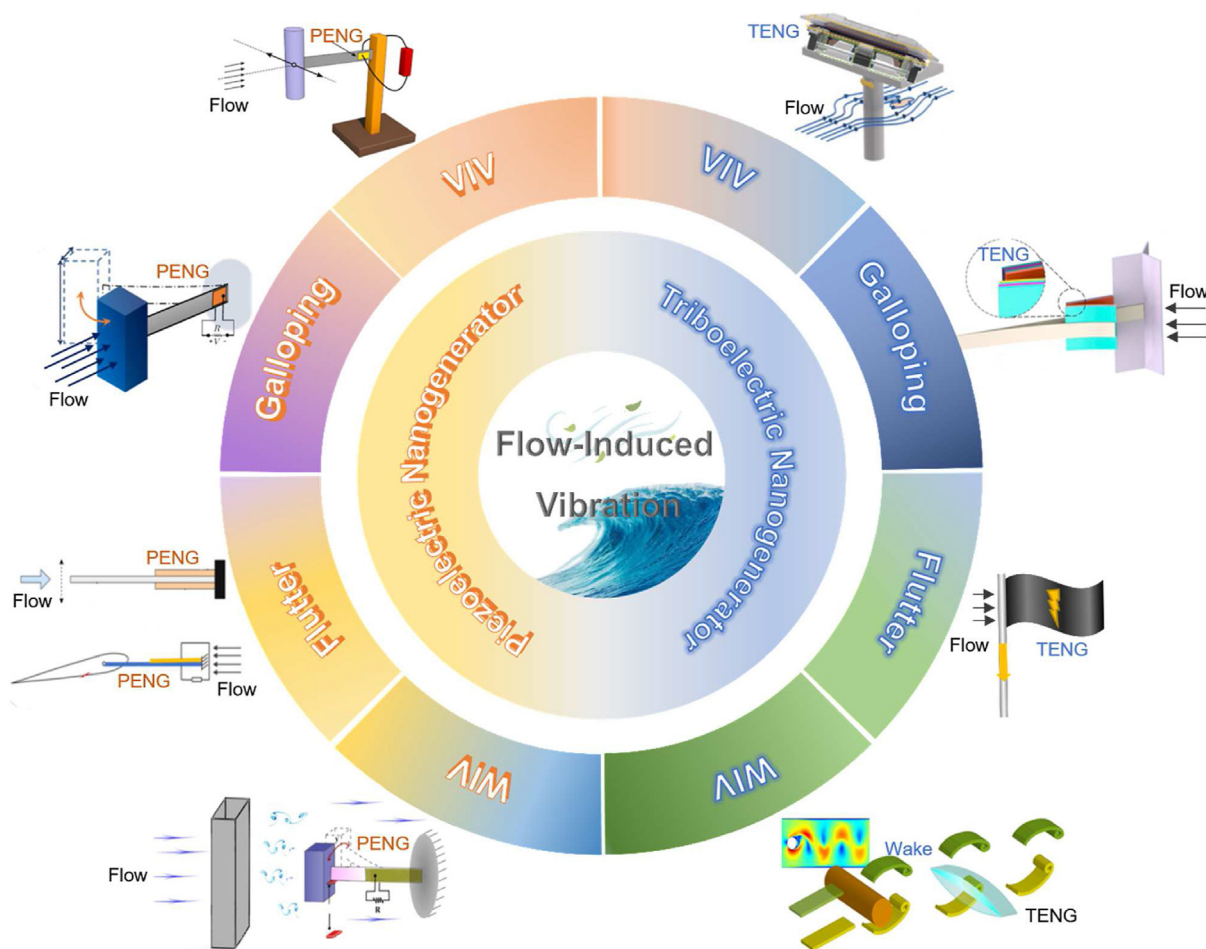


Fig. 1. Overview diagram of Nanogenerators Utilizing Flow-Induced Vibrations. Adapted with permission [97–104]. Copyright 2020, 2021, Elsevier; Copyright 2022, 2022, Wiley; Copyright 2014, 2016, AIP; Copyright 2022, American Chemical Society. Open Access from Ref. [99], Published on Micromachines, 2020.

energy through distinct physical principles. PENGs convert mechanical energy, such as vibrations and deformations, into electrical energy through the piezoelectric effect [105–108]. TENGs operate based on the triboelectric effect, which involves the generation of potential difference through the contact and separation of different materials with varying electron affinities, enabling it to be harnessed as electrical energy [109–111]. The vibration phenomenon induced by fluid motion can transform the kinetic energy present in fluid flow into useable mechanical energy. Through appropriate design, efficient energy conversion can be achieved by coupling fluid dynamics, mechanical components, and electrical systems. This section will give a brief overview of the nanogenerator's power generation principle and the mechanism of flow-induced vibration.

2.1. Principle of piezoelectric nanogenerators (PENGs)

The piezoelectric effect was first discovered by the Curie brothers in 1880 in tourmaline, and it is a phenomenon where a material generates charge separation under mechanical stress or deformation. This effect can be categorized into the positive piezoelectric effect and the inverse piezoelectric effect. The positive piezoelectric effect involves the conversion of mechanical energy into electrical energy, whereas the inverse piezoelectric effect involves the conversion of electrical energy into mechanical energy. This article primarily pertains to the application of flow-induced vibration, wherein PENGs precisely exploit the positive piezoelectric effect to convert

mechanical vibration or stress into electrical energy, employing intricately designed piezoelectric materials (Fig. 2(a)).

In piezoelectric nanogenerator technology, piezoelectric materials constitute a crucial component. These materials possess distinctive crystal structures, enabling them to undergo slight deformations when being subjected to external mechanical stress, leading to phenomena of charge separation and potential difference. Let us probe into this process in more detail (see Fig. 2(b)), using zinc oxide (ZnO), a prevalent piezoelectric material, as an example. When an external mechanical stress is applied (such as tension or compression) to ZnO crystals, the internal lattice structure of the crystal undergoes slight deformation. This deformation leads to the separation of positive and negative charges within the crystal, as alterations in the crystal structure impact the distribution of electrons. Positive charges accumulate in one region of the crystal, while negative charges accumulate in another, resulting in the formation of a potential difference. This potential difference gives rise to an internal electric field force that influences the distribution of electrons within the material. Electrons undergo displacement due to the influence of the electric field force, leading to a reconfiguration into a novel electron distribution pattern. This rearrangement of electrons results in a modification of the charge distribution throughout the material's interior, giving rise to a potential difference known as the piezoelectric potential. Notably, the piezoelectric potential is not merely a static phenomenon of charge distribution; it is a dynamic process that fluctuates with variations in external mechanical stress. As external stress increases or

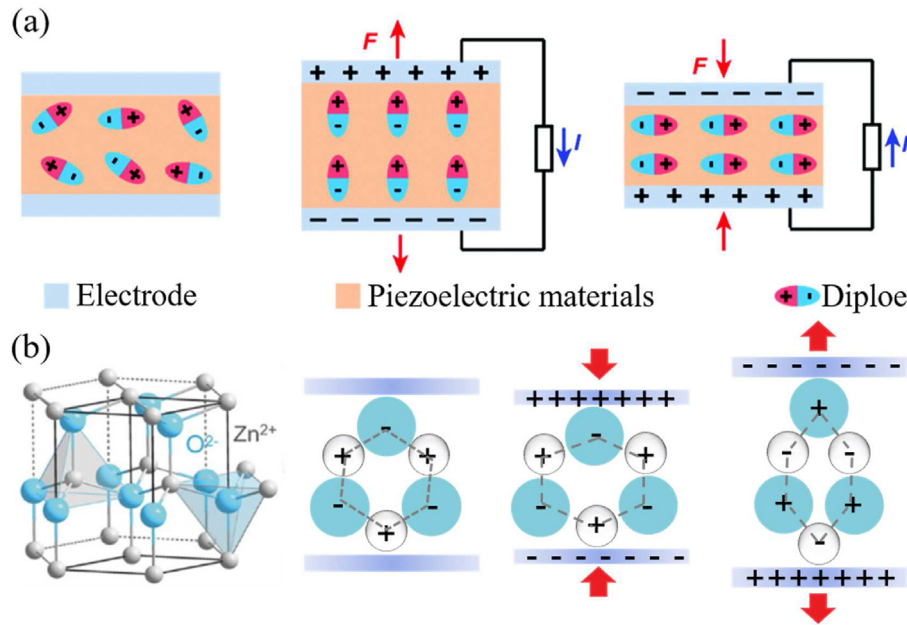


Fig. 2. Electrification principle of PENGs. (a) Positive piezoelectric effect under force. Adapted with permission [112]. Copyright 2020, Royal Society of Chemistry. (b) Lattice structure changes inside ZnO under external mechanical stress Adapted with permission [113]. Copyright 2018, AIP.

decreases, the potential difference correspondingly amplifies or diminishes. This capability allows piezoelectric materials to generate continuous variation in potential under mechanical strain, producing a measurable charge output. This charge output can be employed to drive external circuits, such as charging batteries or other electronic devices, facilitating energy conversion and storage. This characteristic bestows upon piezoelectric nanogenerator technology potential significance in various applications, such as powering small electronic devices using energy generated from wind and ocean sources.

For quantitatively describing anisotropic piezoelectric materials, the piezoelectric equations and constitutive equations under small and uniform mechanical strains are given below [114]:

$$P_i = (e)_{ijk}(s)_{jk} \quad (1)$$

$$\begin{cases} T = c_E s - e^T E \\ D = e s + k E \end{cases} \quad (2)$$

where ' s ' represents mechanical strain; $(e)_{ijk}$ is the third-order piezoelectric tensor. ' T ' and ' c_E ' are stress and elastic tensors, respectively; ' k ' is the dielectric tensor. The displacement current generated by dielectric polarization is:

$$J_D = \frac{\partial P_s}{\partial t} = e_{ijk} \left(\frac{\partial s}{\partial t} \right)_{jk} \quad (3)$$

Equation (3) expresses the rate of change of the applied strain with the piezoelectric nanogenerator proportional to the output current.

The displacement current is the current generated within the nanogenerator. In the absence of an external electric field, the displacement field is the polarization field density $D_z = P_z = \sigma_p(z)$ in the medium. The displacement current is:

$$J_{Dz} = \frac{\partial P_z}{\partial t} = \frac{\partial \sigma_p(z)}{\partial t} \quad (4)$$

Equation (4) represents the rate of change of surface polarized

charges, which corresponds to the observed output current of the piezoelectric nanogenerator.

For the external circuit, the open-circuit voltage of the piezoelectric nanogenerator is $V_{oc} = z\sigma_p(z)/\epsilon$. Due to the presence of an external load ' R ', the current output equation of the piezoelectric nanogenerator is

$$RA \frac{d\sigma}{dt} = z[\sigma_p(z) - \sigma(t)] / \epsilon \quad (5)$$

In Equation (5), ' A ' represents the electrode surface area. In cases where the applied strain varies relatively slowly, ' z ' becomes a function of time ' t '.

2.2. Electrification principle of triboelectric nanogenerators (TENGs)

The principle of electricity generation in the TENG originates from the triboelectric effect, which is a phenomenon based on the movement of electrons between materials. When different materials come into contact and separate due to friction under the action of an external force, the difference in electron affinities leads one material to lose electrons and carry a positive charge, while the other material gains electrons and carries a negative charge. Based on this principle, mechanical energy can be converted into electrical energy.

In order to elucidate the phenomenon of Contact Electrification between different types of materials, Wang et al. [115] proposed the electron cloud/potential model based on fundamental electron cloud interactions (Fig. 3) to encompass a broader range of material systems. This model aims to address the challenges faced by traditional surface state models in explaining cases such as metal-polymer and polymer-polymer interactions. This model focuses on the formation and interaction of electron clouds, localizing electrons within specific atoms or molecules in materials, occupying specific atomic or molecular orbitals. In this model, an atom of a material can be envisioned as a potential well, where outer electrons are loosely confined within the potential well, forming the electron cloud of the atom or molecule. Parameters in the model

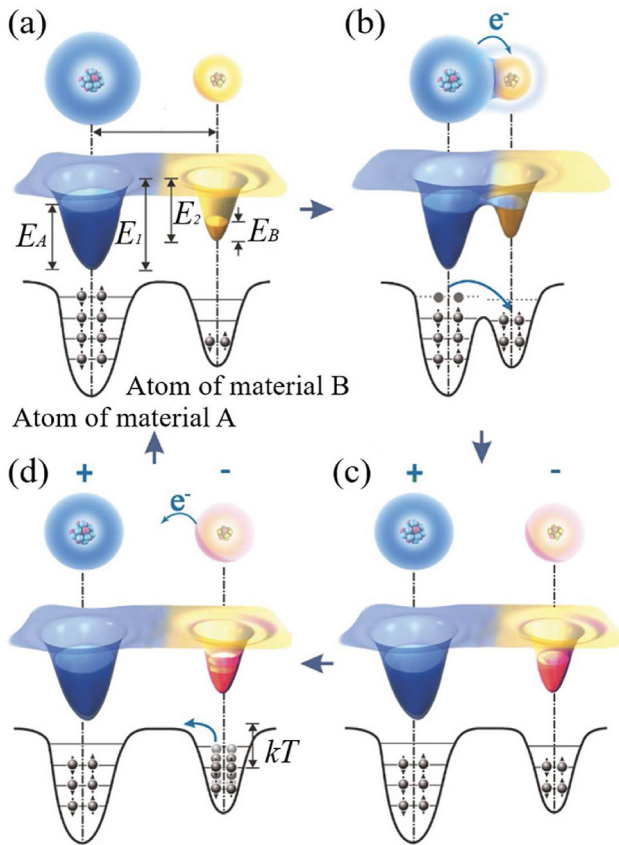


Fig. 3. Electron cloud potential well model, schematic diagram of electron cloud and potential energy profile. Two atoms belonging to two materials, A and B, respectively, when they are: (a) before contact, (b) in contact, and (c) after contact, showing electron transfer from one atom forcing electrons to overlap to the other. (d) The charge release of the atoms at elevated temperature T once kT approaches the barrier height. Variables: d , the distance between two points in the nucleus; E_A and E_B , the energy levels occupied by electrons; E_1 and E_2 , the potential energy escape of electrons; k , the Boltzmann constant; T , the temperature. Adapted with permission [115]. Copyright 2018, Wiley.

encompass the distance between electron clouds (d), the occupied energy levels of electrons in atoms A and B (E_A and E_B), and the potential energy required for electrons to escape from the surfaces of materials A and B (E_1 and E_2). Fig. 3(a) shows that, before the two materials come into contact, due to the localized trapping effect of the potential well, electrons are confined within the well and unable to move freely. However, when materials A and B make contact, physical contact introduces a 'shielding' effect, causing an overlap of the electron clouds. This leads to the transformation of the initial single potential well into an asymmetric double potential well, thus creating the opportunity for electrons to jump from atoms of material A to atoms of material B (see Fig. 3(b)). As shown in Fig. 3(c), after the separation of the two materials, if the temperature is not too high, most of the electrons transferred to material B will be retained due to the energy barrier E_2 in material B. This results in the separation of electrons, leading to material A carrying a positive charge and material B carrying a negative charge, thereby producing the triboelectric effect. Fig. 3(d) illustrates the process of charge release at an elevated temperature T . As temperature increases and the value of kT rises, the energy fluctuations of electrons become more pronounced. Consequently, electrons are more prone to escape the potential well, either returning to the atoms they originally belonged to or being released into the air. This model further explains why the

electrons generated by the triboelectric effect can be sustained, as energy barriers exist in various types of materials.

In addition to the above qualitative explanations, the process of triboelectrification also has a solid theoretical basis. The driving force of TENG is the Maxwell displacement current, which is caused by the time-varying electric field and polarization of the dielectric. In the case of TENG, friction charges are generated on the surface due to the Contact Electrification between two different materials. To explain the contribution of contact-induced static charges in the Maxwell equation, Wang [114] added an additional term, P_s , to the displacement vector D , called mechanical-driven polarization, i.e.

$$\mathbf{D} = \epsilon_0 \mathbf{E} + \mathbf{P} + \mathbf{P}_s \quad (6)$$

Here, the polarization vector P is due to the presence of an external electric field, while the additional term, P_s , is mainly due to the presence of surface charges that are independent of the relative motion between the electric field and the dielectric. Substituting equation (6) into the Maxwell equation group and defining [116,117].

$$\mathbf{D}' = \epsilon_0 \mathbf{E} + \mathbf{P} \quad (7)$$

can reformulate the Maxwell's equations as:

$$\nabla \cdot \mathbf{D}' = \rho_f - \nabla \cdot \mathbf{P}_s \quad (8a)$$

$$\nabla \cdot \mathbf{B} = 0 \quad (8b)$$

$$\nabla \times \mathbf{E} = -\frac{\partial \mathbf{B}}{\partial t} \quad (8c)$$

$$\nabla \times \mathbf{H} = \mathbf{J} + \frac{\partial \mathbf{P}_s}{\partial t} + \frac{\partial \mathbf{D}'}{\partial t} \quad (8d)$$

In equation (8d), $\frac{\partial \mathbf{D}'}{\partial t}$ represents the displacement current caused by the time-varying electric field and the electric field-induced dielectric polarization; $\frac{\partial \mathbf{P}_s}{\partial t}$ is due to the displacement current caused by an external strain field that is non-electric in nature. The first term dominates at high frequencies, such as those used in wireless communications, while the second term is responsible for energy generation at low frequencies or quasi-static conditions. The contribution of TENG's output current is related to the driving force of the $\frac{\partial \mathbf{P}_s}{\partial t}$ term in the displacement current, which is referred to as the Wang term. In general, these two terms can be approximately decoupled and treated independently. However, if the external triggering frequency is high, $\frac{\partial \mathbf{D}'}{\partial t}$ and $\frac{\partial \mathbf{P}_s}{\partial t}$ can effectively couple, and interference between the two can be significant, which may occur in the MHz to GHz range.

2.3. Mechanism of flow-induced vibration

The energy harvested from flow-induced vibrations has emerged as a transformative paradigm within the realm of renewable energy, capitalizing on the intricate dynamics of fluid-structure interaction to harness mechanical energy from fluid flows and convert it into useable electrical power. This innovative approach holds the potential to address the ever-increasing demand for sustainable energy sources while mitigating environmental concerns. The mechanism of flow-induced vibration serves as the cornerstone of this concept, embodying the complex interplay between fluid motion and solid structures.

The phenomenon of flow-induced vibration arises from the dynamic interaction between a fluid and a solid structure when

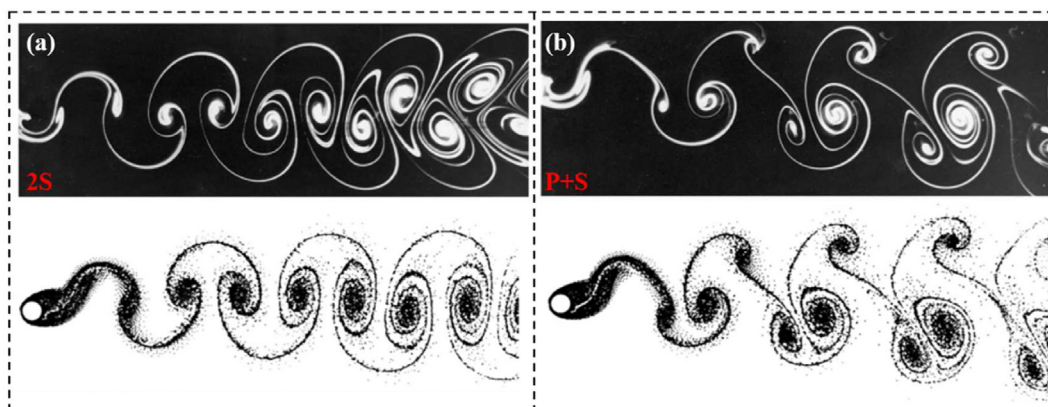


Fig. 4. Experimental visualization and numerical simulation results of two typical vortex modes: (a) 2S and (b) P + S. Adapted with permission [120]. Copyright 2004, Annual Reviews.

subjected to fluid flows. This interaction leads to the generation of mechanical vibrations or oscillations in the structure, primarily driven by the exchange of momentum and energy between the fluid and the solid surface. At the core of this mechanism lies the fluid-structure interaction (FSI), where the fluid's flow characteristics and the structure's mechanical properties mutually influence each other, resulting in a dynamic response that can manifest as vibrations, oscillations, or even deformations. One of the primary contributors to flow-induced vibration is the phenomenon of vortex shedding [118,119]. When a fluid flows past a bluff body or a structure with a significant cross-sectional area perpendicular to the flow direction, vortices are shed from the downstream side of the structure. These vortices create alternating pressure zones, inducing periodic changes in the forces exerted on the structure. Fig. 4 shows two typical eddy shedding modes [120]. This phenomenon, known as vortex-induced vibration, can lead to pronounced mechanical oscillations and even structural fatigue over time. The vortex-induced vibration has been extensively studied in various engineering applications, such as bridges [121], offshore platforms [122], and underwater pipelines [123], where its effects can be critical to the structural integrity and safety of these systems. Furthermore, in aerodynamic applications such as aircraft wings [124], wind turbine blades [125], and aerospace structures [126], flow-induced vibrations can be significantly influenced by aeroelastic effects. Aero-elasticity refers to the coupling between aerodynamic forces and structural dynamics, which can lead to self-excited oscillations and even instability in the presence of specific flow conditions. Aeroelastic flutter is a classic example of this interaction, where the aerodynamic forces induced by the flow interact with the structure's natural frequencies, resulting in sustainable oscillations. Non-linear dynamics further enrich the complexity of flow-induced vibrations. Fluid-structure interactions often exhibit non-linear behaviors due to variations in fluid properties, such as viscosity, or non-linear structural responses under varying load conditions. These non-linear effects can lead to intricate phenomena, including mode interactions, frequency detuning, and bifurcations, making accurate prediction and analysis of flow-induced vibrations challenging [127].

As shown in Fig. 5, the common forms of flow-induced vibrations can be primarily categorized into four types: vortex-induced vibration (VIV), galloping, flutter, and wake-induced vibration (WIV). VIV occurs when fluid flows around a bluff body, leading to the formation of alternating vortices in the wake, which in turn induces periodic lateral vibrations of the object. This phenomenon typically occurs within a Reynolds number range from several hundreds to thousands and relies on the Strouhal number to

predict the shedding frequency of the vortices. VIV is particularly significant in marine engineering, such as in the vibrations of risers on offshore oil platforms, and it is also utilized in energy harvesting, where the kinetic energy of the vibrations is converted into electrical energy. Galloping occurs when the separation point of the fluid on the windward face of a structure moves with the vibration, generating an asymmetric aerodynamic force and causing transverse vibration. This type of vibration is common in power lines under icy conditions, as well as in the design of bridges and high-rise buildings. Its vibration frequency is usually lower than that of VIV, with larger amplitudes. In the field of energy harvesting, specially designed galloping devices can operate at low wind speeds, providing a stable energy output. Flutter is a self-excited vibration phenomenon that arises when the pressure distribution on the surface of a solid changes due to fluid flow, causing the structure to undergo torsional and bending vibrations. In energy harvesting, the two main forms of flutter used are: (1) the flapping of flexible films under flow; and (2) the flutter of airfoils induced by fluid. The onset of flutter is related to the elasticity of the structure, mass distribution, fluid velocity, and its relative angle to the structure. Flutter is particularly crucial in aeronautical engineering, such as wing flutter in aircraft, and in wind energy conversion systems, structures designed to harness flutter can enhance the efficiency of energy capture. Wake-induced vibration occurs when the wake of an upstream object affects a downstream object, especially when both are in the path of the fluid flow. The vortices shed from the upstream object induce vibrations in the downstream object. This phenomenon is commonly observed in arrays of structures, such as groups of wind turbines or clusters of buildings. Wake-induced vibration must be specially considered in the design of energy harvesting systems to prevent potential resonance damage.

Each flow-induced vibration mechanism for energy harvesting presents unique advantages and challenges. VIV offers broad applicability across a wide range of Reynolds numbers, making it suitable for marine engineering and converting kinetic energy from vibrations into electrical energy, with effective utilization of low-speed fluid dynamic power. However, its vibration frequency and amplitude are subject to the limitations imposed by flow speed and object shape, necessitating specific conditions for vortex shedding frequency prediction. Galloping is advantageous for stable operation at low wind speeds and is particularly relevant under adverse weather conditions, such as icing, capable of generating large amplitude transverse vibrations. Its main drawback is the typically lower frequency compared to VIV, which can lead to significant structural stress and fatigue, requiring careful design to avoid

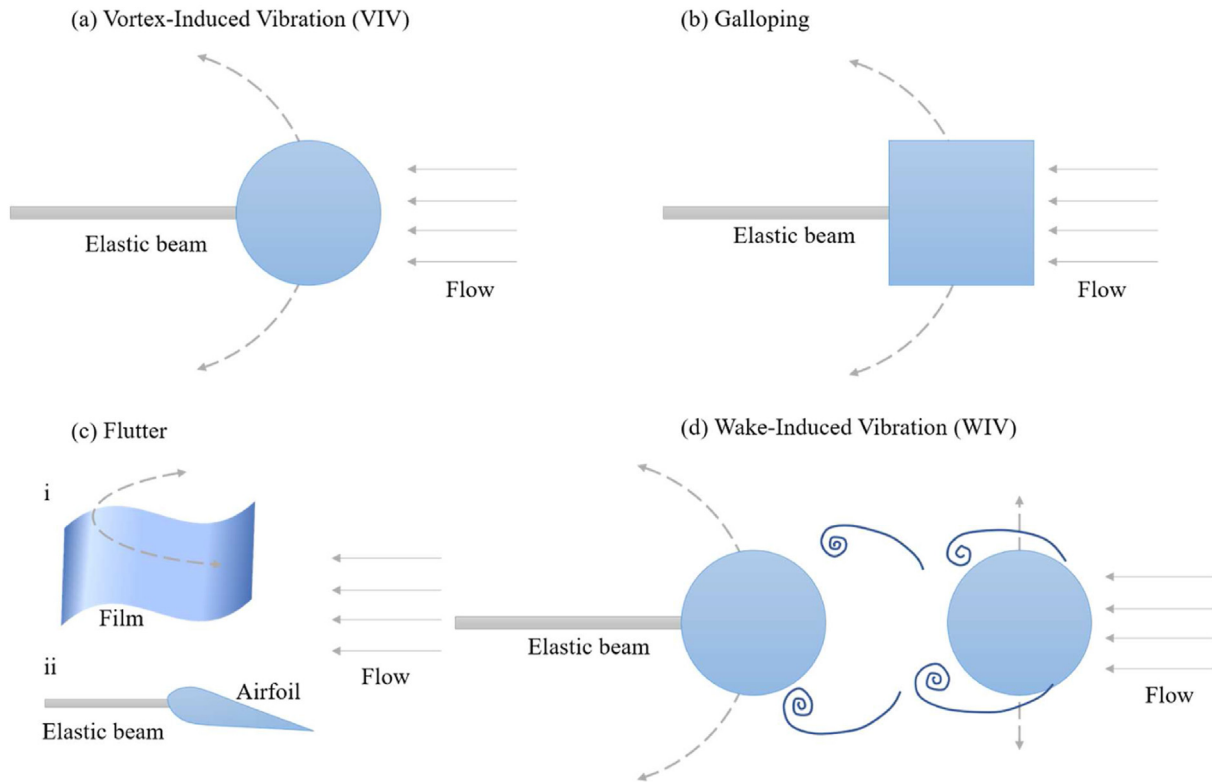


Fig. 5. Four classic forms of flow-induced vibration (a) vortex-induced vibration (b) galloping (c) flutter (d) wake-induced vibration.

destructive vibrations. Flutter, on the other hand, utilizes torsional and bending vibrations and is especially useful in aeronautical engineering and wind energy conversion systems, potentially greatly enhancing energy capture efficiency under specific conditions. However, its initiation depends on various factors including structural elasticity, mass distribution, fluid velocity, and angle, making design and optimization complex and demanding on materials and structure. WIV is common in arrays of structures and can extract energy in complex flow fields, but it necessitates special design considerations to prevent resonance damage due to wake effects from upstream objects, with strict requirements on layout and spacing. Selecting the appropriate vibration mechanism for energy harvesting requires a comprehensive consideration based on the specific application environment and objectives.

3. Piezoelectric nanogenerators (PENGs) driven by flow-induced vibrations

The continuous development of energy harvesting technology has sparked interest in micro energy supply solutions, and among them, PENGs utilizing fluid-induced vibrations as a mechanical energy source are gradually showing tremendous potential. The research in this field focuses on driving the deformation of piezoelectric materials by capturing the vibrations generated by fluid flow, thereby converting mechanical energy into electrical energy. In this section, we will focus on how PENGs utilize fluid-induced vibrations to achieve energy harvesting, with special emphasis on various mechanisms such as vortex-induced vibration, galloping, flutter, and wake-induced vibrations (Fig. 6).

3.1. Vortex-induced vibrations

The vortex-induced vibration (VIV), as a fluid-induced mechanical energy source, can be utilized to drive piezoelectric

nanogenerators. By affixing piezoelectric materials onto the vibrating object, the deformation of the material will lead to charge separation, thereby achieving the collection of electrical energy. In recent years, VIV has attracted the attention of researchers, and its potential applications in fields such as ocean engineering, wind energy utilization, and self-powered sensors have gradually emerged [128–130]. As shown in Fig. 7(a), the typical structure of a VIV based piezoelectric energy harvester includes a cylinder, a cantilever beam, and a piezoelectric sensor adhered to the base of the beam [97]. In this complex and sophisticated system, various components work closely together to achieve the efficient conversion of mechanical energy into electrical energy. This aerodynamic force not only induces vibrations in the cylinder but also serves as the driving force for the entire system motion. Especially under certain fluid flow conditions, the phenomenon of VIV occurs, wherein vortices form as fluid flows around the cylinder trigger vibrations in the cylinder. The cantilever beam, as a component connected to the cylinder, plays a crucial role in energy transfer and conversion. When the cylinder vibrates due to the aerodynamic forces, the cantilever beam resonates and follows the vibration, thereby transmitting mechanical energy to other parts of the beam. This process not only requires the cantilever beam to possess a certain level of flexibility and stiffness but also demands the beam to maintain a certain stability during the vibration process, ensuring the efficient transfer of mechanical energy. When the cantilever beam vibrates, the piezoelectric piece also undergoes deformation. Due to the presence of the piezoelectric effect, this deformation leads to charge separation and accumulation, resulting in a potential difference. This potential difference is the result of the conversion of mechanical energy into electrical energy. Zhang et al. [97] investigated the impact of Reynolds numbers ranging from 500 to 33,000 on the piezoelectric energy harvesting from VIV in a circular cylinder. They found that the Reynolds number not only influences the level of energy harvested but also affects the global

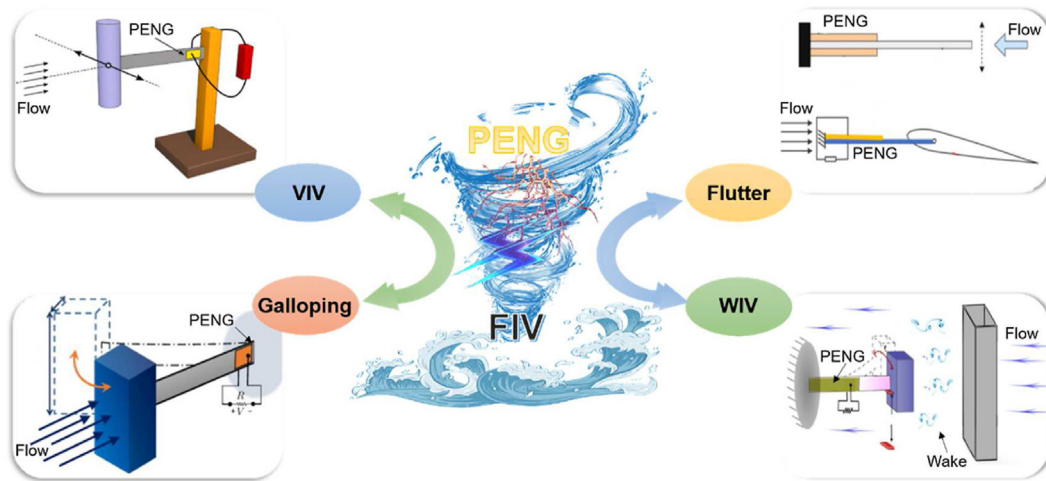


Fig. 6. Schematic of PENG utilizing flow-induced vibrations.

branches of the bifurcation diagram. The results further revealed that for cases with low mechanical damping ratios, the performance of the VIV-based piezoelectric energy harvester is more sensitive to variations in the Reynolds number.

Wang et al. [131] introduced a novel non-contact VIV based piezoelectric wind energy harvester, Fig. 7(b), which differs significantly from most existing VIV based piezoelectric wind energy harvesters. The latter explored the VIV wind energy collection involving embedded composite piezoelectric sensors within the cylinder shell, enabling direct interaction between the piezoelectric cantilever beam and the airflow. The device employs a sealed cylindrical shell design to isolate the piezoelectric material from the erosive effects of the fluid and utilizes a structure that has been bent beforehand to ensure that the piezoelectric plate is subjected only to unidirectional compressive stress. These measures help to extend the lifespan of the piezoelectric plate, effectively enhancing reliability and environmental adaptability. Their results indicated that at a wind speed of 40.0 m/s and a transducer mass of 65 g, the maximum power recorded was 1.438 mW in the form of a single piezoelectric beam that has been bent beforehand. Furthermore, the non-contact piezoelectric wind energy harvester was found to operate effectively over a wide range of wind speeds, from 5.5 m/s to 40.0 m/s (namely a wind speed bandwidth of 34.5 m/s), when using an output voltage of 5 V as the reference value. Furthermore, to address the challenges of high vortex-induced oscillation initiation wind speeds, susceptibility to suppression, and poor rebound characteristics, Fan et al. [132] proposed an elemental surface design for both compact and loose vortex-induced oscillation wind energy harvesting systems, as depicted in Fig. 7(c). Zhu et al. [133] suggested improving the cylinder's response amplitude by affixing fin-shaped stripes onto the cylinder's surface. Fig. 7(d) depicts the flow simulation before and after the installation of the fin-shaped stripes, indicating an increase in fluid dynamic forces. The resistance increased by 27.29% while the lift force rose by 66.01%. Although the flow wakes behind smooth and rough cylinders both exhibits pronounced three-dimensional characteristics, the flow wake becomes notably broader when the cylinder's local roughness is increased. The heightened fluid forces and expanded flow wakes contribute to the enhancement of VIV. Employing magnetic coupling to enhance VIV for energy harvesting is also a common approach, as shown in Fig. 7(e) [134]. Incorporating magnets during the cylinder's oscillation process enables the device to possess five equilibrium points. The stiffness characteristics of the device vary around these equilibrium points, with corresponding ranges of

operational wind speeds, facilitating wind energy collection. Furthermore, it is notable that under varying initial conditions, Tandem vibrational induced vibration energy harvesters could exhibit multiple vibration trajectories at the same wind speed. When vibrating on a high-energy trajectory, the collector's output voltage is relatively higher, thereby improving energy collection efficiency. Sun et al. [135] attempted to combine cylindrical and different shapes (such as square cylinders) and discovered that the device would exhibit both vortex-induced oscillation and galloping (to be introduced in section 3.2). This synergy between the two modes can enhance energy collection efficiency. The average power output of the proposed bluff body design across the entire relevant wind speed range increased by 75% compared to a traditional square cross-sectional bluff body. Remarkably, at a wind speed of approximately 2.95 m/s, the maximum power lift rate observed was 193%. Moreover, they depicted the dynamic behavior with wind speed variation as shown in Fig. 7(f). Further details can be found in reference [135].

3.2. Galloping

Galloping can generate significant motion amplitudes and energy output. Such fluid-induced vibrations can be utilized to excite PENGs, converting mechanical energy into electrical energy through the piezoelectric effect [136–139]. Fig. 8(a) shows the typical structure of galloping, where a square (non-circular) bluff body is connected at the free end of a piezoelectric cantilever beam [98]. When the flow velocity exceeds the device's startup wind speed, it induces transverse beam oscillations and stretches the piezoelectric element, generating an electrical signal. Similarly, to enhance the energy harvesting performance of this structure, it is common practice to add small structures on the surface. Wang et al. [140] attempted to add small protruding cylinders on the surface of the square column, see Fig. 8(b). The results indicate that, compared to the conventional Galloping-PEH, the proposed galloping piezoelectric energy harvester exhibited a significant increase in performance, with the maximum vibration displacement and maximum output voltage enhanced by 26.81% and 26.14%, respectively. Fig. 8(c) displays various different structures, from left to right: (1) bluff body with a triangular cross-section; (2) T-shaped; and (3) fork-shaped [141–143]. However, enhancing non-linear effects may also pose challenges, such as more complex dynamic behaviors, frequency jumps, and non-linear interference.

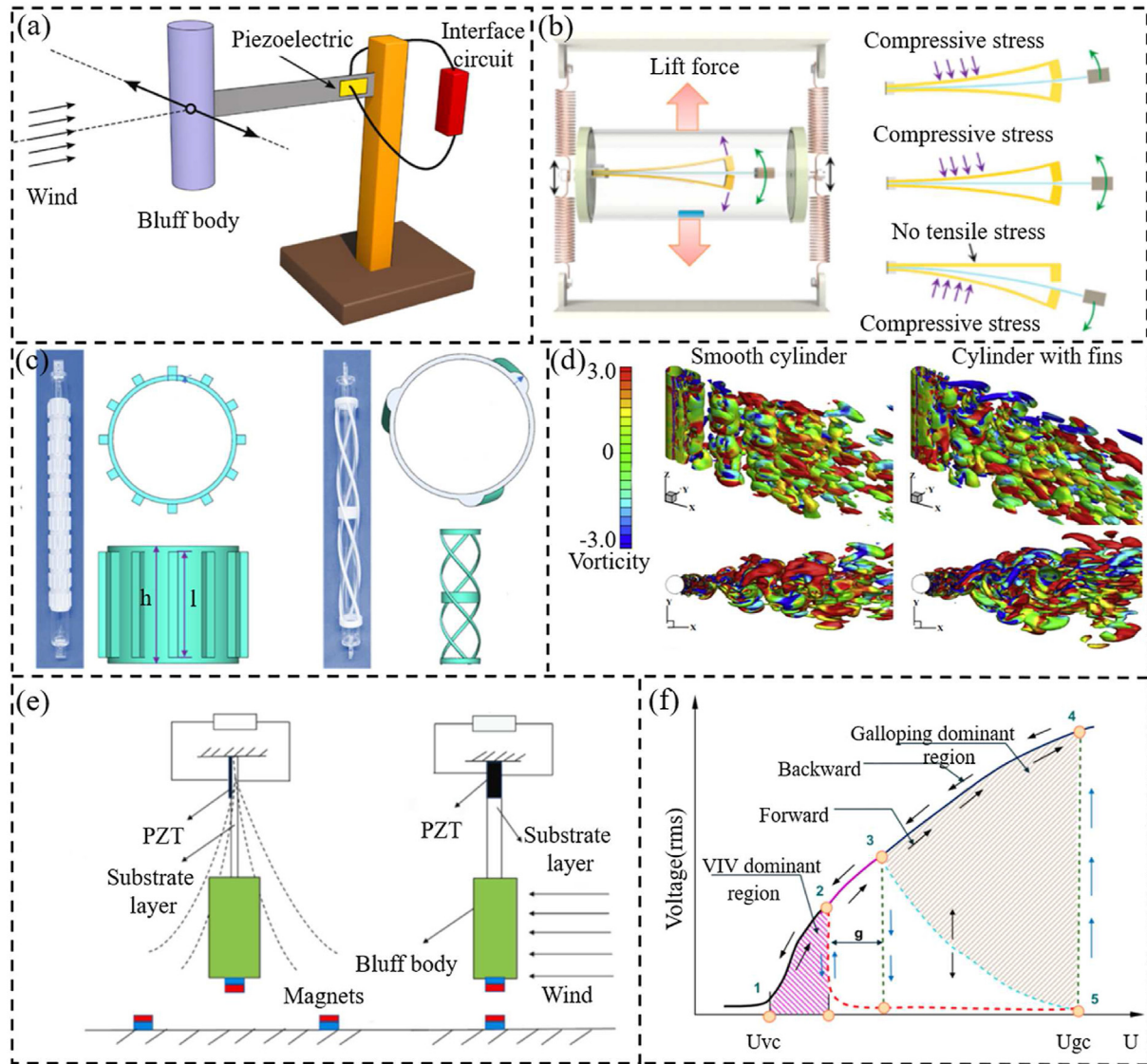


Fig. 7. Utilization of VIV phenomenon by PENGs. (a) Typical structure of vortex induced vibration piezoelectric energy harvester. Adapted with permission [97]. Copyright 2021, Elsevier. (b) Non-contact vortex-induced vibration piezoelectric wind energy harvester. Adapted with permission [131]. Copyright 2021, Elsevier. (c) Response amplitude of cylinder enhanced by fin-like stripes. Adapted with permission [132]. Copyright 2022, Elsevier. (d) Flow simulation before and after installation of fin-like stripes. Adapted with permission [133]. Copyright 2018, Elsevier. (e) Magnetic coupling to enhance vortex-induced vibration. Adapted with permission [134]. Copyright 2023, Elsevier. (f) Dynamic behavior of the vibration energy harvester as the wind speed changes. Adapted with permission [135]. Copyright 2019, Elsevier.

Therefore, when designing and optimizing fluid flow energy harvesting systems, a careful consideration of the pros and cons of non-linear effects is necessary. It is crucial to select appropriate methods to control and manage these effects in order to achieve the optimal energy capture performance. Apart from altering the bluff body's shape, Hu et al. [144] proposed a comb-like beam structure (Fig. 8(d)). The results indicate that, compared to traditional beam design, the initial wind speed of the comb-shaped beam decreased from 2.24 m/s to 1.96 m/s, and under the optimal impedance, the power output at a specific wind speed (3 m/s) increased by approximately 171.2%. Furthermore, similar to VIV, the efficiency in energy collection can also be effectively enhanced by adding magnets. The tri-stable non-linear energy harvesting device shown in Fig. 8(e) exhibits significant advantages in collecting high-performance energy [145,146]. For the dual-beam piezoelectric energy collector, introducing mutual repulsion of magnets induces bi-stable non-linearity, which is advantageous for reducing critical wind speeds and enhancing output voltage.

3.3. Flutter

When wind passes over structures such as flags and leaves, flutter can trigger unstable vibrations in objects, generating high-frequency mechanical energy [147,148]. This phenomenon can also be applied to PENGs, converting mechanical vibrations into electrical energy. Flutter phenomena hold significance in the design of engineering structures and wind energy utilization. Its integration with PENGs applications offers novel possibilities for the field of sustainable energy. Fig. 9(a) illustrates two typical flapping structures: flag-shaped and airfoil-shaped. When the wind speed exceeds the critical velocity, it triggers the onset of structural instability and generates flapping motion [99,100]. This flapping motion drives the motion of the piezoelectric patch, converting mechanical energy into electrical energy. For the piezoelectric beam equipped with an airfoil, as the flow speed increases, the self-excited motion occurs when the structural damping is insufficient to suppress the motion induced by aerodynamic effects. As shown

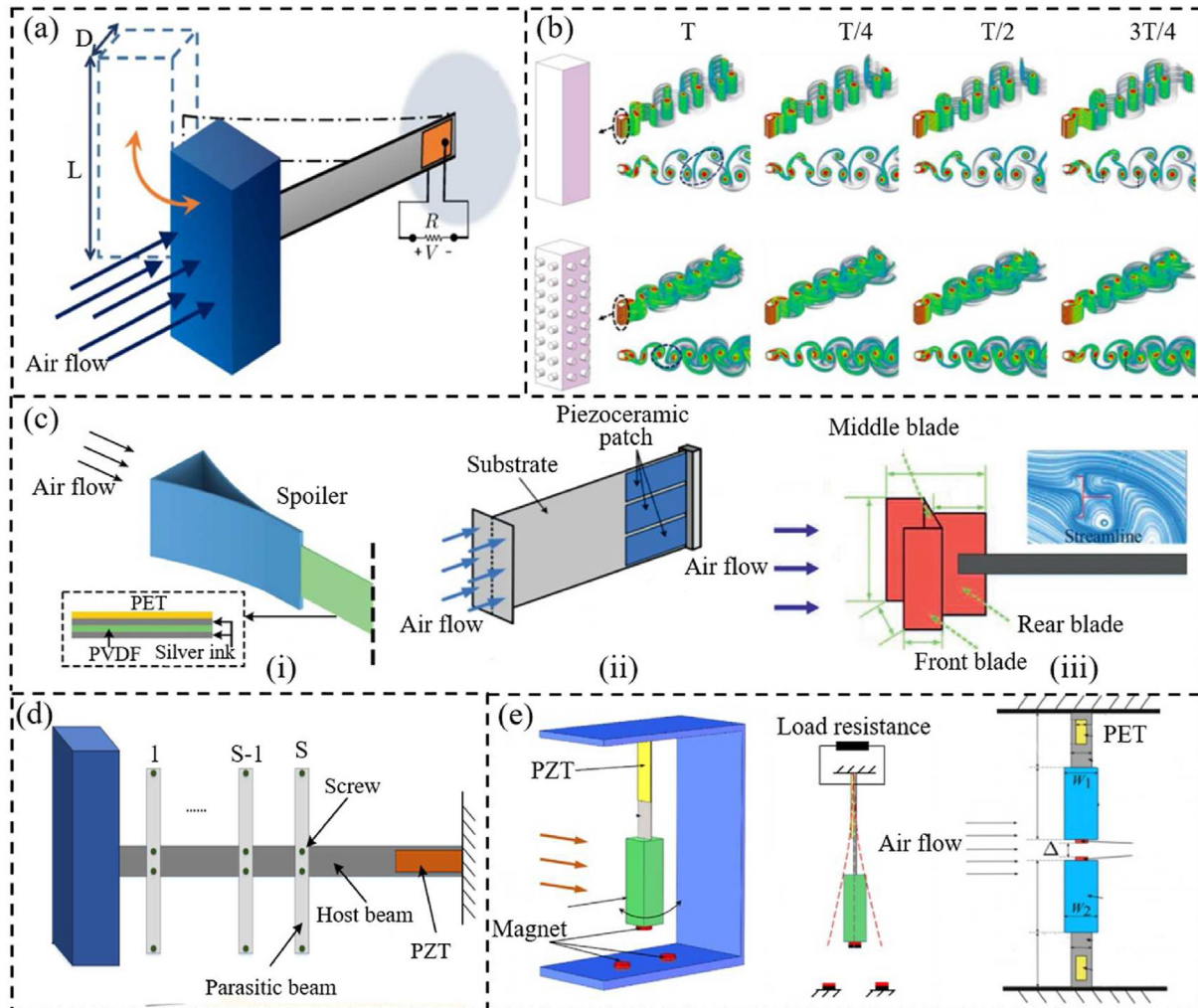


Fig. 8. Utilization of galloping phenomenon by PENGs. (a) Typical structure of galloping. Adapted with permission [98]. Copyright 2014, AIP. (b) Comparison of the flow field before and after adding a small convex column on the surface of the square column. Adapted with permission [140]. Copyright 2021, Elsevier. (c) Three bluff body structures. Adapted with permission [141–143]. Copyright 2010, 2020, AIP. Copyright 2019, Elsevier. (d) Comb beam structure. Adapted with permission [144]. Copyright 2021, Elsevier. (e) Magnetic coupling to enhance galloping. Adapted with permission [145,146]. Copyright 2019, AIP.

in Fig. 9(b), an increase in velocity results in supercritical or subcritical bifurcations [149]. For supercritical instability, the collector's response is stable for any perturbation or initial conditions below and above the critical flutter speed. When the flow speed exceeds the critical flutter speed, due to the presence of structural/aerodynamic non-linearity, limited cycle oscillations occur. In the case of subcritical instability, the collector's response below or near the critical flutter speed is highly dependent on initial conditions or any potential disturbances. In such cases, a sudden jump to larger limit cycle oscillation amplitudes occurs. When the flow speed is greater than the critical flutter speed, the system's response is unaffected by any disturbances.

The flag-shaped structure shown in Fig. 9(c) is commonly employed for harvesting environmental energy, providing power to outdoor microelectronic devices. Agarwal et al. [150] attempted to add various flow obstacles upstream of the flag-shaped structure. They found that in all configurations tested, the D-shaped body induced flutter at the lowest flow velocity of 5.1 m/s. This represents a significant reduction of 50% when compared to the benchmark case, where flutter occurred at a flow velocity of 10.2 m/s without an upstream body. In addition, D-shaped, square, and triangular flow obstacles exhibited yield gains of 11.4 times, 6.7

times, and 4.6 times, respectively, in terms of the output-to-input power ratio compared to the baseline. Inspired by the movement of eels in nature, Taylor et al. [151] proposed the concept of an eel-inspired generator, depicted in Fig. 9(d), which employs piezoelectric polymers to convert mechanical flow energy in oceans and rivers into electricity. Using the periodic vortex path generated by the flow obstacle to stretch the piezoelectric elements, the resulting undulating motion resembles the natural swimming movement of eels. An internal battery stores excess energy generated by the eel-inspired generator, catering to later use by small unmanned monitoring sensors or robots. The flutter behavior of the film depicted in Fig. 9(c) and (d) exhibits a self-excited vibration, meaning it does not require an external periodic force; the structure itself can produce continuous oscillation under the influence of the fluid. While there is a blunt body upstream of the flexible film, the primary cause of the film's flutter is due to the dynamic interaction between the fluid and the film, rather than being solely driven by wake instability. Therefore, categorizing the phenomenon of a flexible film, attached behind a cylinder and exhibiting flutter behavior, as flutter is more appropriate. Orrego et al. [152] conducted tests with inverted flexible piezoelectric films under various parameters (Fig. 9(e)). They found that in a laboratory

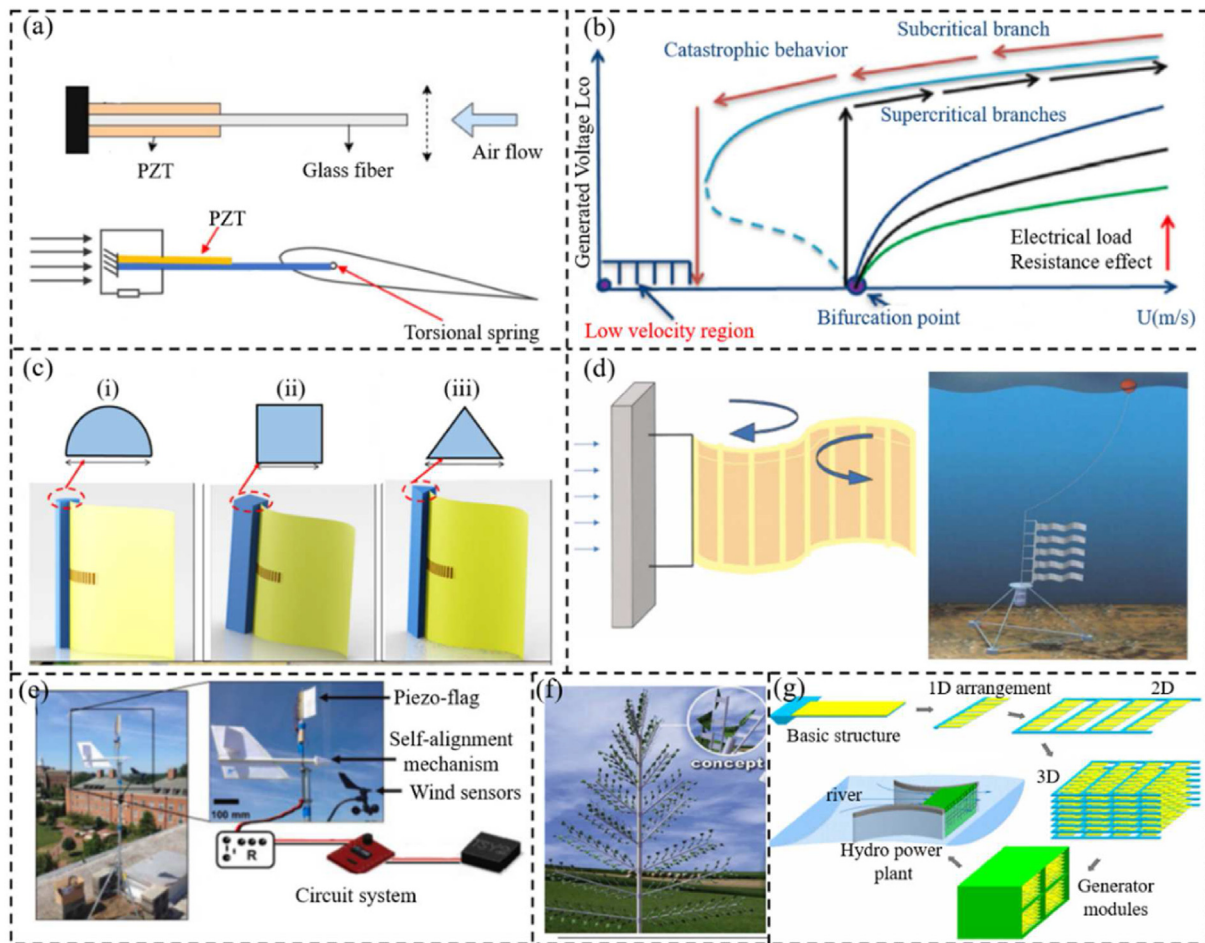


Fig. 9. Utilization of flutter phenomenon by PENGs. (a) Two typical flapping structures: flag-shaped and airfoil-shaped. Adapted with permission [99,100]. Open Access from Ref. [99] Published on Micromachines, 2020. Copyright 2022, Wiley (b) Zoning map as a function of speed. Adapted with permission [149]. Copyright 2016, Elsevier. (c) Flag-shaped structure for harvesting ambient energy. Adapted with permission [150]. Copyright 2023, Springer. (d) Generator of the eel concept. Adapted with permission [151]. Copyright 2001, IEEE. (e) Flexible piezoelectric film for harvesting ambient wind energy. Adapted with permission [152]. Copyright 2017, Elsevier. (f) Leaf-shaped PENG. Adapted with permission [153]. Copyright 2016, Elsevier. (g) Piezo film array to harvest water flow energy. Adapted with permission [154]. Copyright 2004, IEEE.

environment with a wind speed of 9 m/s, the peak electrical power reached around 5.0 mW/cm^3 . Even within the low wind speed range suitable for collecting environmental wind energy (approximately 3.5 m/s), a sustained electricity generation capability (around 0.4 mW/cm^3) was demonstrated. The 'inverted flag' method also uses a self-alignment mechanism to compensate for changes in wind direction, significantly improving the system's operational stability and efficiency under environmental conditions. Additionally, they carried out outdoor experiments, harnessing environmental wind energy to power temperature sensors without the need for energy storage batteries. These exciting results provide optimism for the practical application of this generation method. The concept of biomimetic deployable flutter energy harvesters was initially proposed by Dickson [153]. He envisioned a tree-like structure comprised of potentially hundreds of 'leafstalk' piezoelectric collectors, as depicted in Fig. 9(f). This concept has given rise to a plethora of research articles exploring this structure. To render such small-scale power generation units more practical, it is necessary to operate multiple small generating units in parallel. Fig. 9(g) illustrates an arrangement utilizing piezoelectric films to harvest energy from water flow [154]. First, the power-generating bilayer materials can be arranged together to form a flow conduit, where multiple power generation modules share a flow disturbance. Second, several of these one-dimensional arrangements can

be positioned in a matrix-like manner along the average flow direction. By integrating these power generation matrices with rectifiers, miniature hydroelectric modules can be developed. Theoretical calculations suggest that the PZT-bimorph design is capable of achieving a power output of approximately $6.81 \mu\text{W}$ per element within a volume of 100 mm^3 . This translates to a power density of approximately 68.1 W/m^3 .

3.4. Wake-induced vibrations

Instabilities in the wake can induce vibration in an object, generating mechanical energy. This mechanical energy can be converted into electrical energy through the piezoelectric effect, enabling self-powering. WIV finds significant applications in aerodynamics, hydrodynamics, and marine engineering. The integration of this phenomenon with PENGs presents a novel avenue for energy harvesting in microdevices [155–157]. As shown in Fig. 10(a), the piezoelectric WIV flow energy collector consists of a mechanical oscillator and a portion coupled with an energy collection circuit through piezoelectric components [101]. The oscillator is located downstream of a cylinder or obstacle. As an initial laminar fluid flows past the obstacle, the Karman vortex street forms at the trailing edge, leading to the symmetry breaking. The periodicity of the vortex shedding results in alternating

pressures, thereby generating cyclic lift on the mechanical oscillator. To enhance the energy collection efficiency, Alhadidi et al. [101] also employed magnetic coupling, as mentioned previously, to broaden its response bandwidth. Hu et al. [158] proposed a piezoelectric energy harvester that attaches a thin oscillating blade to the free end of a beam (Fig. 10(b)). They adjusted the natural frequency of the oscillator by altering its dimensions and shape using magnets affixed to the top and bottom surfaces of the blade. This arrangement provides sufficient space for the shed vortices to emanate from the cylinder, exciting the oscillating blade and aligning the oscillator's natural frequency with the shedding frequency of the synchronized vortices. Eventually, based on this experimental setup, they developed a theoretical model that identifies the optimal positioning, offering valuable insights. As depicted in Fig. 10(c), Zhao et al. [159] introduced a novel hydrodynamic piezoelectric energy collector utilizing WIV. Through frequency analysis, they found that the VIV and the WIV performances are respectively governed by the shedding frequency of wake vortices and the inherent frequency. Moreover, As the distance between obstacles changes, the flow pattern changes significantly, see Fig. 10(d) [159]. For the distance $L \approx 1 \sim 2D$, a small

range is termed (i) the extension region, where no vortices exist in the gap. Here, L is the distance between obstacles and D is the diameter of the obstacles. For distance of approximately $L \approx 2 \sim 5D$, it is termed (ii) reattachment; in this case, only a pair of well-developed vortices exists in the gap. Vortex structures act upon the downstream cylinder surface. Consequently, the fluid shear layer reattaches to the downstream cylinder. When the distance surpasses $5D$, it is labeled (iii) the co-shedding region, featuring fully developed vortex structures within the gap. Experimental results reveal that the maximum power densities achieved by the inverted D-shaped, circular, and D-shaped cylinders are 570.3 W/m^3 , 596.4 W/m^3 , and 1074 W/m^3 , respectively. These values represent increases of 43.2, 25.3, and 31 times over the baseline scenario without wake interference. Furthermore, the optimal experimental spacing ratios for these configurations were found to be 5, 2.6, and 2, respectively. The process of wake-induced vibration is influenced by various conditions, where different shapes and sizes of stationary obstacles generate diverse wake patterns. Simultaneously, the varying distance between the stationary obstacles and the cylinder leads to distinct aerodynamic phenomena around the cylinder. Zhang et al. [160] conducted relevant studies

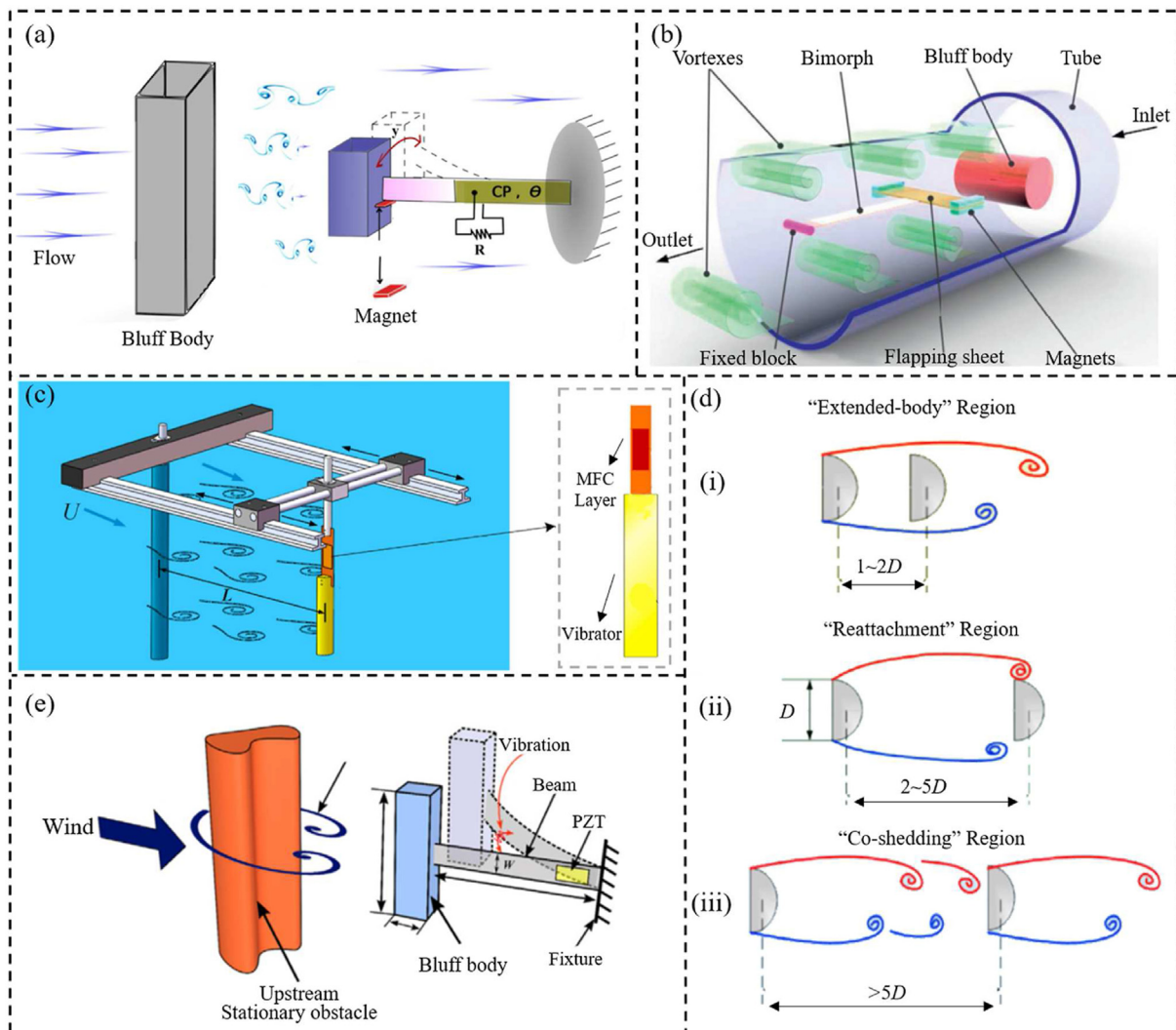


Fig. 10. Utilization of wake-induced vibrations phenomenon by PENGs. (a) Typical structure of wake-induced vibrations. Adapted with permission [101]. Copyright 2016, AIP. (b) Energy harvester with thin vibrating blade structure. Adapted with permission [158]. Copyright 2018, Elsevier. (c) Cylindrical wake-induced vibration. Adapted with permission [159]. Copyright 2021, Elsevier. (d) The change of the flow field when the distance between the bluff bodies is different. Adapted with permission [159]. Copyright 2021, Elsevier. (e) The influence of various condition changes on the flow field. Adapted with permission [160]. Copyright 2021, Elsevier.

by altering the aforementioned three conditions to modify the aerodynamic characteristics around the cylinder, as depicted in Fig. 10(e).

4. Triboelectric nanogenerators (TENGs) driven by flow-induced vibrations

With the advancement of micro-energy harvesting technology, TENGs have emerged as a novel method of energy collection. These devices utilize fluid-induced vibrations to generate mechanical energy, subsequently driving the triboelectric effect to convert mechanical energy into electrical energy. This section will focus primarily on how TENGs utilize fluid-induced vibration for energy harvesting. It will particularly emphasize different mechanisms such as vortex-induced vibration, galloping, flutter, and wake-induced vibrations (Fig. 11).

4.1. Vortex-induced vibrations

In TENGs, the vortex-induced vibration can be utilized to generate mechanical oscillations, thereby triggering the triboelectric effect in TENGs and converting mechanical energy into electrical energy. The application potential of the vortex-induced vibration mechanism becomes progressively prominent in fields such as ocean engineering, wind energy, water flow energy harvesting, and underwater sensors [161–163]. Fig. 12(a) shows a TENG device for harvesting mechanical energy from vortex-induced vibrations in pipes [164]. This device provides mechanical energy to power monitoring systems and enables the realization of sensing and signal transmission. A highly efficient energy collector is established using the contact-separation mode of TENG, converting the mechanical energy from vibrating pipelines into electrical energy. Results showed that the device achieved a peak output power of $14.0 \mu\text{W}$ at a circuit resistance of $200 \text{ M}\Omega$, corresponding to a power density of 5.56 mW/m^2 . The TENG device consists of a friction pair comprised of dielectric material films connected to a mass-spring base, ensuring the contact-separation motion of the friction pair. Experimental tests involving the installation of the TENG device on sample pipelines demonstrate the device's output performance and long-term durability. Kim et al. [102] introduced a TENG device that simultaneously employs the free-support sliding (FS) and contact-separation (CS) modes to collect mechanical energy from oscillations generated by water flow impact on a cylinder (see Fig. 12(b)). They further resolved the critical issue of 'lock-in' phenomenon occurring in traditional cylinder VIV systems by introducing fluid-induced collision between two sidewalls. Due to the presence of two sidewalls, this device exhibits stable electricity generation within a wide flow velocity

range (0.05–1.02 m/s), and the phenomenon of lock-in is absent. Apart from energy harvesting, seals can utilize their whiskers to sense changes in vortices within the flow field, Fig. 12(c), enabling them to identify and locate prey [165]. Inspired by this, Wang et al. [165] designed a TENG sensor mimicking the unique wave-like features of seal whiskers. This device primarily consists of an internal sensing unit, flexible silicone rubber follicles (Dragonskin 00–20), and artificial whiskers (polydimethylsiloxane, PDMS). Its output signal is highly correlated with interactive motion parameters, enabling the determination of the relative movement status of underwater objects. Fig. 12(d) illustrates a fully encapsulated VIV triboelectric nanogenerator designed for wind energy recovery. Unlike most previous wind energy harvesting TENGs, a bouncing PTFE ball is entirely enclosed within a square column in this design [166,167]. This unique design separates the contact electrification process from the external environment, effectively reducing the wear experienced by traditional wind energy harvesting TENGs and improving the stability and reliability of the device. Fig. 12(e) demonstrates a wind energy harvesting device similar in structure to that of Fig. 12(d). Both utilize springs and cylinders to generate VIV. However, the TENG in Fig. 12(e) is composed of a pair of parallel electrode plates [168]. When the cylinder is affected by lateral airflow, it functions as an oscillator, converting wind energy into kinetic energy. Subsequently, the TENG transforms the kinetic energy into electrical energy through the periodic contact and separation actions between the two electrode plates. The results show that when the wind speed is 2.78 m/s , the observed average power output was recorded at $392.72 \mu\text{W}$, with an average power density of 96.79 mW/m^2 .

4.2. Galloping

When the fluid flows through the elastic structure, the resulting galloping motion can also be converted into friction and separation processes in the TENG, thereby generating charges and electrical energy. In nature, when a gentle breeze blows, trees sway, suggesting that tree-like structures can capture the energy of slight wind movement. Inspired by this, Zeng et al. [169] designed a TENG device as shown in Fig. 13(a), where a cantilevered spring steel plate serves as the tree trunk, offering elastic restoring force to maintain the system equilibrium. Simultaneously, the sealed trapezoidal casing resembles the external contour of a tree and serves a dual purpose: on one hand, it effectively captures wind energy through the FIV effect, and on the other hand, the unique design not only segregates the TENG units from the wind-driven components to shield them from environmental disturbances but also circumvents the substantial rotational resistance and frictional wear present in conventional TENG-based wind energy harvesters. Furthermore,

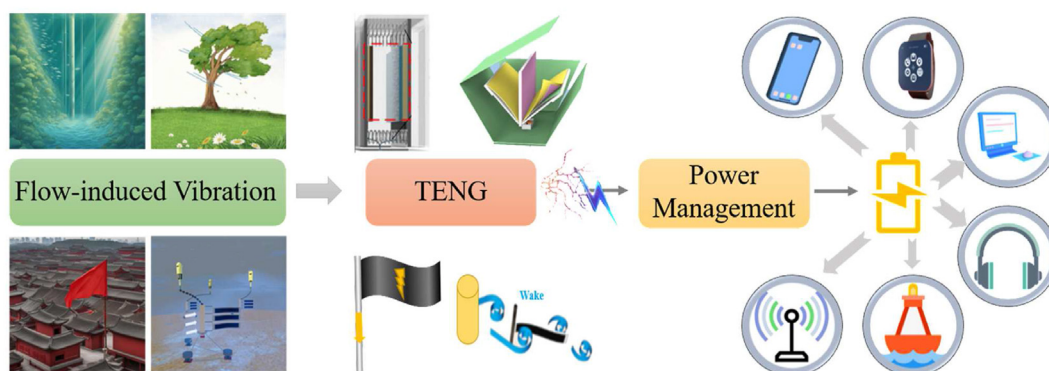


Fig. 11. Schematic of TENG utilizing flow-induced vibrations.

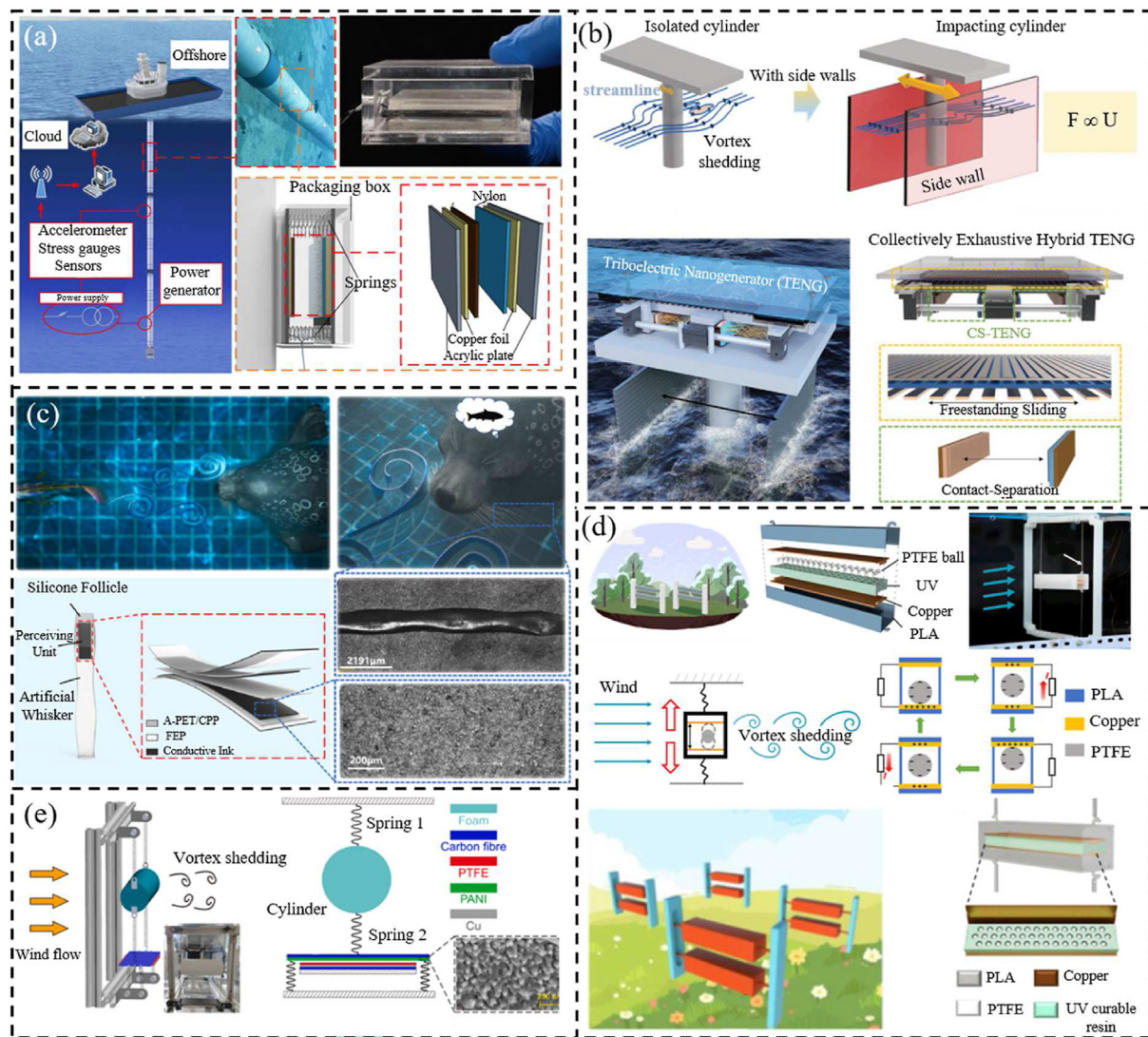


Fig. 12. Utilization of VIV phenomenon by TENGs. (a) Vibrating pipeline energy harvesting device. Open Access from Ref. [164]. Published on Sensors, 2021. (b) Oscillations of water hitting a cylinder (with or without walls). Adapted with permission [102]. Copyright 2022, Wiley. (c) Seal whisker flow sensor. Fully encapsulated vortex-induced vibration triboelectric nanogenerator. Adapted with permission [165]. Copyright 2022, Elsevier. (d) Small ball structure. Adapted with permission [166,167]. Copyright 2022, Springer. Open Access from Ref. [166]. Published on Nanomaterials, 2021. (e) Parallel plate structure. Adapted with permission [168]. Copyright 2022, Elsevier.

based on the concept of array assembly, as this array system expands further, the network of arrays can generate significant power output, rendering it a formidable source of electrical supply. Fig. 13(b) depicts a TENG device inspired by fish caudal fins, where a bluff body-cantilever beam structure is designed [170]. In this arrangement, the beam structure employs soft materials, swaying under the influence of water flow and driving the small sphere within the bluff body to generate electrical signals through surface friction. The triboelectric soft fish tail demonstrates an open-circuit voltage (VOC) ranging from 200 V to 313 V across flow velocities of 0.24–0.89 m/s. Moreover, following a period of 30 days submerged in water, the VOC of the triboelectric soft fish tail (TE-SFT) maintains 96.81% of its initial value. This resilience to water immersion highlights the device's durability and its potential for long-term applications in energy harvesting from aquatic environments. In Fig. 13(c), a square bluff body-flickering beam structure is designed to convert flow velocity into fluctuating vibrations [171,172]. Here, the square bluff body is affixed to a base using a cantilever beam made of spring steel. The TENG comprises a mobile FEP sheet on the bluff body's base and fixed interconnecting electrodes. The oscillatory vibrations of the

bluff body drive the FEP sheet to move on the interconnecting electrodes, generating electric signals via electrostatics. The preload of the FEP sheet can be adjusted by positioning the electrode plates. Additionally, as in the third part, piezoelectric sheets can be attached to the beam to form a composite energy collection mode. Apart from the aforementioned contact mechanisms, employing limited galloping (Fig. 13(d)) also has yielded excellent outcomes for the TENG design [103,173]. This approach also serves to limit the maximum deformation of the beam under high wind speeds, preventing damage and enhancing the device's stability and durability. Simultaneously, it increases the vibration frequency, thereby improving the electromechanical conversion efficiency.

4.3. Flutter

The phenomenon of flutter finds crucial applications in the design of aircraft, wind power generation, and architectural structures. The integration of energy collection with TENGs will introduce novel innovative approaches to the realm of sustainable energy. Flutters exhibit diverse forms, encompassing thin-film

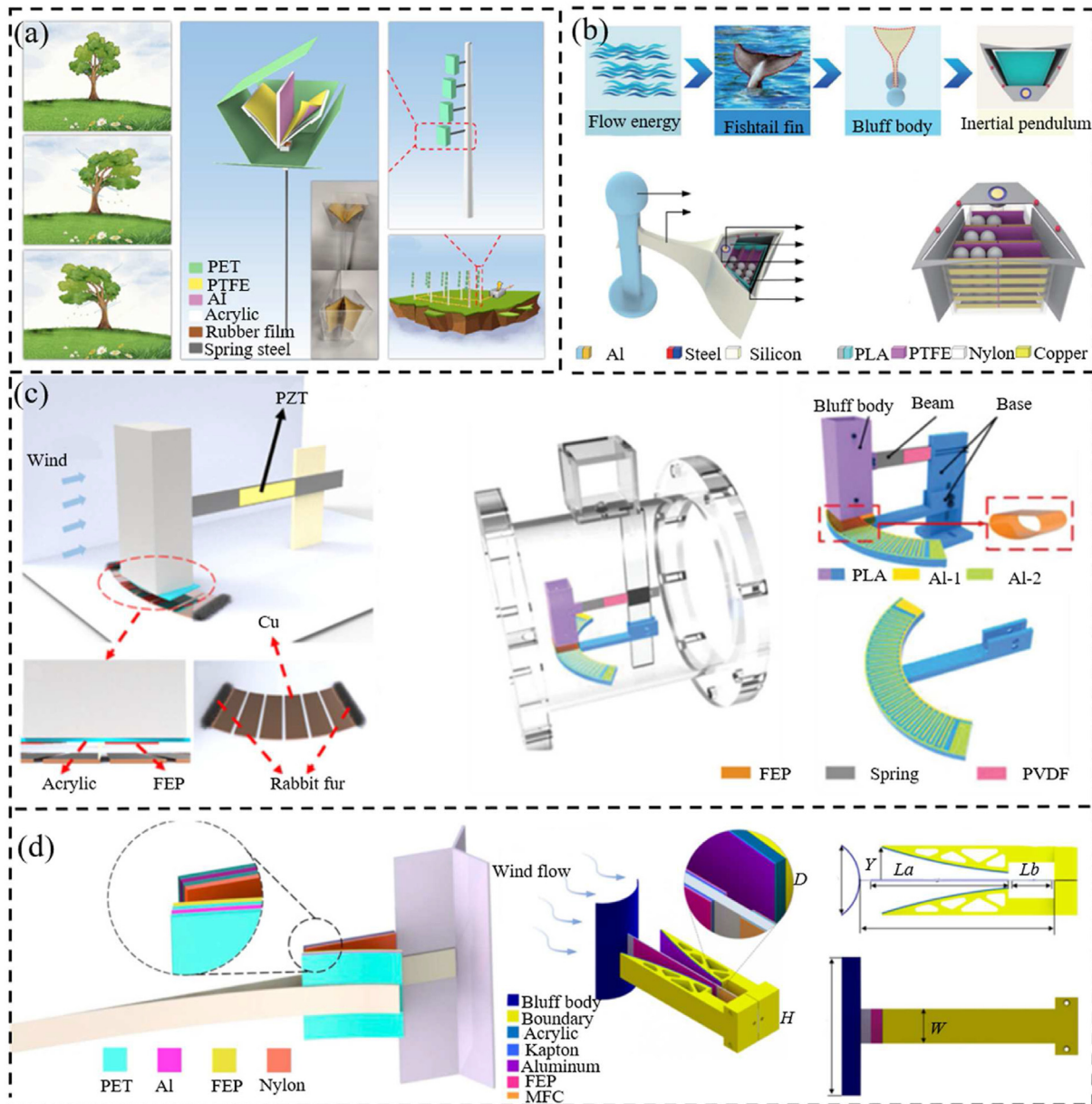


Fig. 13. Utilization of galloping phenomenon by TENGs. (a) Tree structure energy harvester. Adapted with permission [169]. Copyright 2020, Elsevier. (b) Fish tail fin TENG device. Adapted with permission [170]. Copyright 2023, Springer. (c) Blunt body swing friction structure. Adapted with permission [171,172]. Copyright 2022, Wiley. Open access from Ref. [172]. Published on iScience, 2022. (d) Energy harvesters limiting the movement position of the beam. Adapted with permission [103,173]. Copyright 2020, Elsevier. Copyright 2020, AIP.

structures with cavities and flag-shaped structures with one end free and the other end fixed. Inspired by the fascinating characteristics of bi-stable structures, Kim and colleagues [174] introduced a fresh concept based on the phenomenon of periodic rapid flipping, namely, the Periodic Rapid Flipping Triboelectric Nanogenerator, as depicted in Fig. 14(a). Initially, a thin elastic sheet is deformed into a curved shape by adjusting the distance between the two clamped ends of the sheet, which is shorter than its length. When the bent sheet is positioned within a uniform low-speed airflow where its two ends are aligned parallel to the flow, the sheet maintains a state of static equilibrium through a balance among aerodynamic forces, bending forces, and compressive forces acting upon it. With the escalation of the free-stream velocity, the applied aerodynamic forces on the sheet become sufficiently robust to swiftly flip the sheet into an alternate equilibrium state. Due to

the symmetric configuration, if the sheet is continuously exposed to the wind, periodic rapid flipping motion can be achieved. The results demonstrate that an electrode layer, possessing a modest active area of 5 cm by 1 cm, is capable of delivering a maximum output power of 7.3 mW. This performance is achieved at the optimal wall distance, with a free-stream velocity of 9.1 m/s. Furthermore, Phan and colleagues [175] explored using an elastic rubber band between two distinct vibrating thin films (Fig. 14(b)). The aeroelastic vibration induced within the rubber band resulted in substantial oscillations within the thin-film energy harvester, leading to a noteworthy enhancement in electricity generation performance as the rubber band's rapid cyclic amplitude increased. Inspired by the common sight of fluttering flags in daily life, Wang et al. [176] developed a flag-type TENG adaptable to changes in humidity and wind direction, as shown in Fig. 14(c). During the

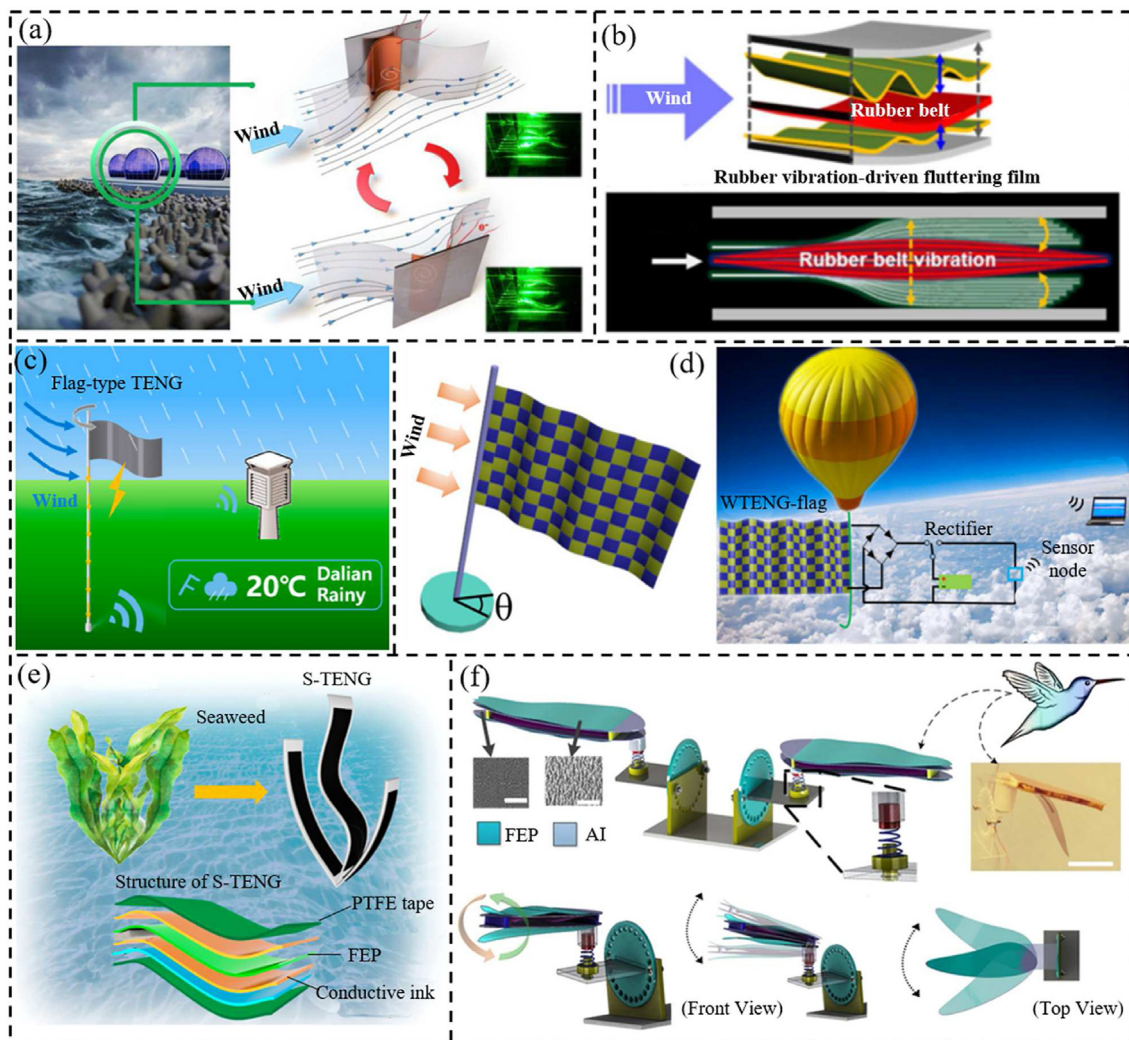


Fig. 14. Utilization of flutter phenomenon by TENGs. (a) Fast flipping triboelectric nanogenerators. Adapted with permission [174]. Copyright 2020, Elsevier. (b) Elastic rubber bands enhance flutter motion. Adapted with permission [175]. Copyright 2017, Elsevier. (c) A flag-type TENG adaptable to changes in humidity and wind direction. Adapted with permission [176]. Copyright 2020, Elsevier. (d) Flexible flag energy harvester. Adapted with permission [177]. Copyright 2016, American Chemical Society. (e) Water flow energy harvester imitating seaweed. Adapted with permission [177]. Copyright 2021, American Chemical Society. (f) Schematic and experimental structure of a hummingbird wind TENG [178]. Copyright 2017, Springer.

process of swaying in the wind, the flag-type TENG causes alternating contact between PTFE and the carbon electrodes on both sides, thus converting wind energy into electrical energy. To enhance device stability, the edges are sealed to isolate the triboelectric layers from air. This isolation ensures the electrical performance of the TENG is independent of relative humidity, addressing common issues of performance degradation under humid conditions and varying wind directions in traditional TENG designs. They also tried two flags placed side by side at intervals and found that a 40-fold increase in power density was observed compared to a single flag-type TENG setup. Under these conditions, with a matched loading resistance of 5 M Ω at a wind speed of 7.5 m/s, a maximum current of 6.8 μ A, and a peak output power of 36.72 μ W were recorded. The generated electrical energy can also power sensor nodes, transmitting weather information to display screens through wireless communication modules. Similarly, as shown in Fig. 14(d), the edges of the two materials can also be directly bonded to form a flag. Inspired by seaweed, Wang et al. [177] introduced a seaweed-mimetic flexible structure TENG, aiming to bend and deform under the influence of water flow or waves (Fig. 14(e)). When the flexible structure undergoes periodic

oscillations due to wave action, the TENG experiences corresponding contact and separation. This design exhibits high output performance and potential adaptability to various water flow conditions, but it is sensitive to environmental factors such as flow velocity, turbulence, and debris. Bio-inspired technologies hold significant potential for harvesting energy from clean and sustainable sources. Drawing inspiration from the hummingbird-wing structure, Ahmed et al. [178] introduced a shape-adaptive, lightweight triboelectric nanogenerator (TENG) aimed at harnessing the unique flutter mechanics of hummingbirds for small-scale wind energy harvesting, as illustrated in Fig. 14(f). They explored flutter mechanics on multiple contact surfaces, employing various independent and lightweight electrification designs. Flutter-driven TENGs were deposited onto simplified wing designs to match electrical performance with variations in wind speed. The hummingbird TENG (H-TENG) device weighed 10 g, making it one of the lightest TENG harvesters in the literature. Further, by employing a hybrid design of six TENG networks, they achieved a peak electrical power output of 1.5 W/m² at a wind speed of 7.5 m/s. Furthermore, it was found that the charging rate increases approximately linearly with the number of TENG collectors involved.

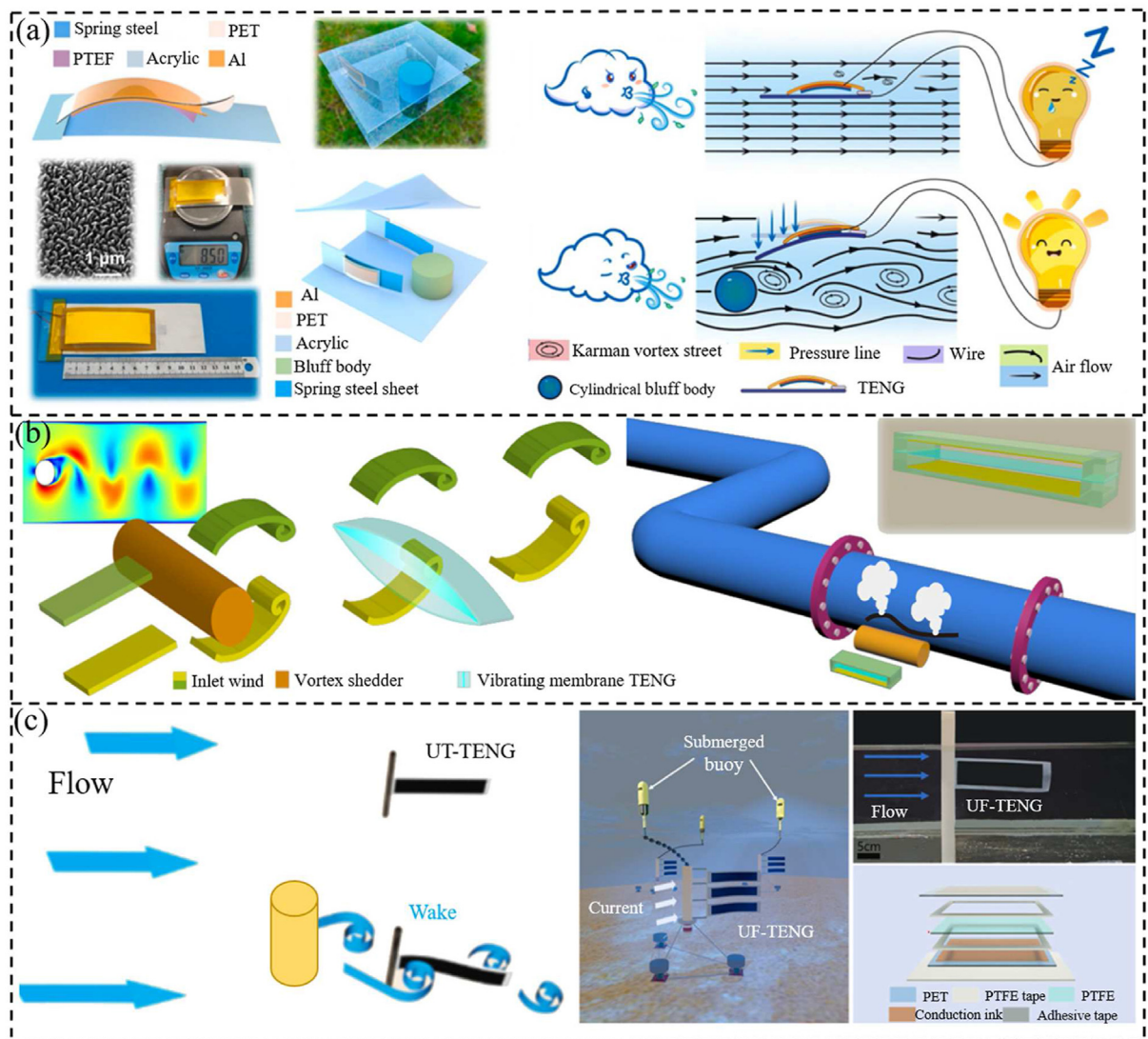


Fig. 15. (a) Blunt bodies to enhance the flutter effect of TENG devices. Adapted with permission [179]. Copyright 2022, Elsevier. (b) Schematic illustration of using Karman vortex street to enhance the vibration of the TENG for ultra-low wind speed energy harvesting and flow sensing. Adapted with permission [104]. Copyright 2022, American Chemical Society. (c) Underwater flag-shaped TENG. Adapted with permission [180]. Copyright 2021, Elsevier.

4.4. Wake-induced vibrations

Vibrations caused by wakes are common in nature and can also be captured using TENG technology and converted into electrical energy. In complex fluid environments such as water or turbulent airflows, wake-induced vibrations provide potential avenues for energy harvesting. As shown in Fig. 15(a), Yuan et al. [179] utilized the wake-galloping effect by placing a bluff body upstream to enhance the flapping effect of the TENG device. This design can capture gentle breeze energy with wind speeds as low as 1.0 m/s, and the straightforward contact-separation design also eases the manufacturing and portability. As a novel strategy, this work holds significant value for the future application of microwind energy harvesting and self-powered systems. Simultaneously, the design of such bluff body structures reminds us to deepen our understanding of the characteristics of energy sources during the process of energy device design; tailoring designs to the attributes of energy sources may yield unexpected outcomes. As shown in Fig. 15(b), Li et al. [104] introduced a wake-driven membrane triboelectric nanogenerator for ultra-low-speed wind energy harvesting and fluid sensing. By incorporating a bluff body in front of

the TENG device, a Karman vortex street was induced, leading to a reduction of the device's cut-in wind speed from 1 m/s to 0.52 m/s. Furthermore, at inlet wind speeds of 1 m/s and 2 m/s, the instantaneous output density of the device was significantly enhanced by 1000-fold and 2.65-fold, respectively. It is worth noting that this work not only provides an ingenious strategy for ultra-low-speed wind energy harvesting but also demonstrates promising prospects for monitoring airflow in natural gas exploration and transportation. Furthermore, most ocean-current-power applications are constrained to relatively high starting ocean current velocities. There is an urgent need for an ocean current energy harvester with lower startup velocities and a broader operational range. To address this need, Wang et al. [180] developed a flexible underwater flag-like triboelectric nanogenerator for harvesting ocean current energy (Fig. 15(c)). They employed a cylindrical structure to induce a Karman vortex street, and the results demonstrated that the wake generated by the bluff body significantly enhanced the vibration of the TENG. This enhancement allowed the flag-shaped TENG to effectively harvest ocean current energy at low current speeds. The Underwater Flow Triboelectric Nanogenerator (UF-TENG) is capable of being induced into vibration by water flows with

velocities ≥ 0.0133 m/s, through the adjustment of its bending stiffness to $K_B \leq 0.65 \times 10^{-4}$. Furthermore, experimental investigations conducted in a circulating water flume revealed that the UF-TENG, featuring a mass ratio of 1590, exhibits superior output performance. Notably, a peak output power of $52.3 \mu\text{W}$ was recorded using an assembly of six UF-TENG units at a flow velocity of 0.461 m/s, highlighting the potential of this design for enhanced energy harvesting in underwater environments.

5. Comparison of piezoelectric and triboelectric nanogenerators

The emergence of piezoelectric and triboelectric nanogenerators (PENG and TENG) as novel energy harvesting technologies has sparked significant interest in the scientific and engineering communities. These two technologies aim to convert mechanical energy into electrical energy to meet the ever-growing energy demands and provide sustainable energy solutions. Despite sharing a common objective, PENG and TENG exhibit significant differences in principles, applications, advantages, and disadvantages. In this section, we compare the similarities and differences of these two approaches in Fig. 16, facilitating researchers to make diversified choices based on their characteristics to address distinct energy harvesting and sensing needs.

First, in terms of the working principle, PENG is a technology based on the piezoelectric effect, which is pronounced in certain specific materials. When these materials are subjected to mechanical stress or deformation, they undergo charge separation, leading to the generation of an electric potential difference. However, TENG utilizes the triboelectric effect, inducing charge transfer through friction and separation between two distinct materials. The generation of this electric potential difference provides the necessary conditions for subsequent energy conversion. Therefore, the materials they employ are also different. PENG typically utilizes mature piezoelectric materials such as quartz, lead zirconium titanate (PZT), and polyvinylidene fluoride (PVDF). In contrast, TENG requires carefully selected materials to achieve efficient charge separation effects. Common friction materials include polydimethylsiloxane (PDMS), polytetrafluoroethylene (PTFE), as well as conductive materials like metals. The frictional characteristics of these materials play a crucial role in the operation of TENG. Furthermore, in terms of mechanical input, PENG primarily relies on specific mechanical deformations, such as bending, pressure, or vibration, to generate potential differences and currents. Its design needs to consider how to efficiently apply mechanical stress to achieve effective energy conversion. On the other hand, TENG is distinct; its working principle involves periodic contact and separation between two materials. This enables TENG to harvest energy from a wide range of mechanical motions, such as light tapping, sliding, and even subtle vibrations from the natural environment.

In terms of application areas, both PENG and TENG show potential in energy harvesting. PENG excels in scenarios requiring precise mechanical deformations, such as collecting energy from controlled mechanical strains. It holds promising applications in self-powered sensors, health monitoring devices, and other fields. In contrast, TENG is suitable for a variety of mechanical motions, whether it is human movement, natural environmental vibrations, or friction from everyday activities. This grants TENG a wide range of potential applications in wearable devices, smart homes, environmental monitoring, and more. In terms of advantages and disadvantages, PENG benefits from its mature piezoelectric materials and principles, enabling efficient energy conversion under specific mechanical conditions. However, PENG requires precise mechanical deformations and is constrained by specific strain directions, which might lead to fatigue issues in certain situations. In contrast, TENG possesses the advantage of generating energy from a wide range of mechanical movements and is less reliant on specific mechanical deformations, thus offering greater design flexibility. However, to achieve efficient triboelectric effects, TENG requires careful selection of suitable materials, and the relatively low current produced by TENG is also a significant drawback.

To clarify the distinction between the two types of nanogenerators and provide a coherent comparison, Table 1 delineates the performance characteristics of the materials employed in PENGs and TENGs under various flow-induced vibration modes. The comparison of triboelectric nanogenerators (TENGs) and piezoelectric nanogenerators (PENGs) is drawn from the data in Table 1, which benchmarks their energy harvesting efficiencies, material compositions, operational conditions, and the resultant power outputs. This comparison aims to illuminate the unique operational advantages and potential application scenarios of each nanogenerator type based on the observed performance metrics. TENGs typically utilize a wider variety of materials compared to PENGs, including common metals, polymers, and composites. The operational principle of TENGs is based on contact electrification and electrostatic induction, which allows them to operate effectively at lower frequencies and velocities, as observed in the table. TENGs demonstrate substantial power output at lower velocities, which is beneficial in environments where wind or water flow is inconsistent or slow. PENGs, on the other hand, are primarily constructed from piezoelectric materials such as PZT, MFC, and PVDF. They operate based on the piezoelectric effect, where mechanical stress induces an electrical charge in the material. PENGs in Table 1 show a strong dependence on the frequency and amplitude of vibrations for energy conversion. They often yield higher power outputs at higher frequencies and velocities, suggesting they are more suited to environments with more consistent and strong mechanical disturbances. When comparing VIV-induced energy harvesting, PENGs show a tendency to generate higher power outputs at increased velocities, while TENGs provide

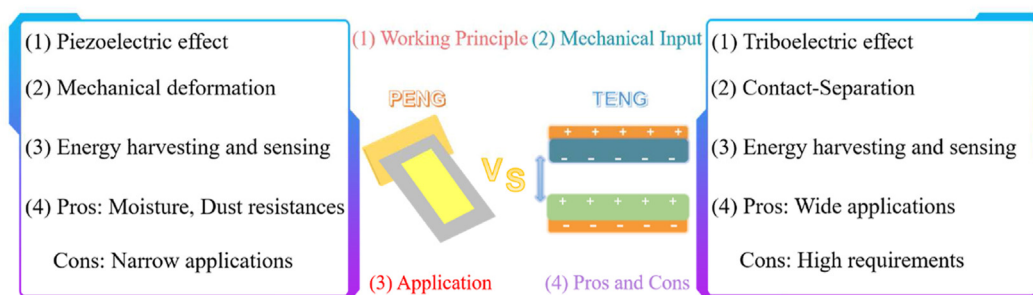


Fig. 16. Comparison of PENG and TENG.

Table 1
Performance comparison of PENG and TENG.

Nanogenerators	Type	Materials	Velocity/frequency	Output	Refs.
PENG	VIV	PZT	40 m/s	2.87 mW	[131]
PENG	VIV	MFC	2 m/s	1.2 mW	[181]
PENG	VIV	MFC	10 m/s	1.2 mW	[182]
PENG	Galloping	PZT	5 m/s	143.6 μ W	[140]
PENG	Galloping	PZT	4 m/s	4 mW	[142]
PENG	Galloping	PZT	3 m/s	0.12 mW	[144]
PENG	Flutter	PZT	40 m/s	6.72 mW	[99]
PENG	Flutter	MFC	5 m/s	1.16 mW	[150]
PENG	Flutter	PVDF	9 m/s	5 mW/cm ³	[152]
PENG	WIV	MFC	6 m/s	5 mW	[101]
PENG	WIV	PZT	0.75 m/s	0.37 mW	[158]
PENG	WIV	MFC	0.65 m/s	1074 W/m ³	[159]
TENG	VIV	Copper/PTFE	29.5 m/s	62.2 W/m ²	[167]
TENG	VIV	PANI/PTFE	2.78 m/s	96.79 mW/m ²	[168]
TENG	VIV	Si/LV polymers	1.02 m/s	21.8 mW/m ³	[102]
TENG	Galloping	Al/FEP	14 m/s	0.13 mW	[103]
TENG	Galloping	Nylon/PTFE	0.89 m/s	5.56 W/m ³	[170]
TENG	Galloping	PVDF/FEP	10 m/s	2.08 mW/m ²	[172]
TENG	Flutter	Carbon/PTFE	7.5 m/s	36.72 μ W	[179]
TENG	Flutter	Ni/Kapton	14 m/s	135 mW/kg	[183]
TENG	Flutter	Resin/Nylon	4 m/s	3.64 W/m ³	[184]
TENG	WIV	Steel/PTFE	1.8 m/s	149 mW/m ²	[179]
TENG	WIV	Copper/PDMS	2 m/s	26 mW/m ²	[104]
TENG	WIV	Conductive ink/PTFE	0.461 m/s	52.3 μ W	[180]

more consistent output across a range of velocities. This implies that for applications involving variable flow rates, TENGs might be more reliable, whereas PENGs could be more efficient in a steady flow environment. Furthermore, in the context of material performance, PZT-based nanogenerators frequently exhibit higher power output compared to those made from other materials, indicating that PZT's material properties are highly conducive to energy harvesting. In summary, the choice between TENG and PENG for a specific application would depend on the operational environment and the desired energy output. TENGs may be preferable for low-frequency, variable flow scenarios, while PENGs might be chosen for their efficiency in high-frequency, consistent flow conditions.

6. Challenges and future perspectives

Despite significant progress in the field of nanogenerators utilizing flow-induced vibrations, there are still challenges to be addressed in order to fully exploit the potential of these energy

harvesting devices. Key challenges reside in the stability and durability of materials used in these nanogenerators, their coupling with fluids, and their interaction with the environment, as illustrated in Fig. 17. Harsh and dynamic operating environments of these devices result in material degradation over time, thereby impacting their long-term performance. Developing materials capable of withstanding these conditions and maintaining their performance over an extended period is a crucial aspect in advancing this field. Another potential challenge lies in the need for standardization and normalization of performance parameters. Various types of nanogenerators employ diverse metrics to quantify their efficiency and energy conversion capabilities, making direct comparisons challenging.

6.1. Challenges faced by TENGs and PENGs

It is worth noting that when discussing PENG and TENG technologies, it is crucial to pay special attention to the significant

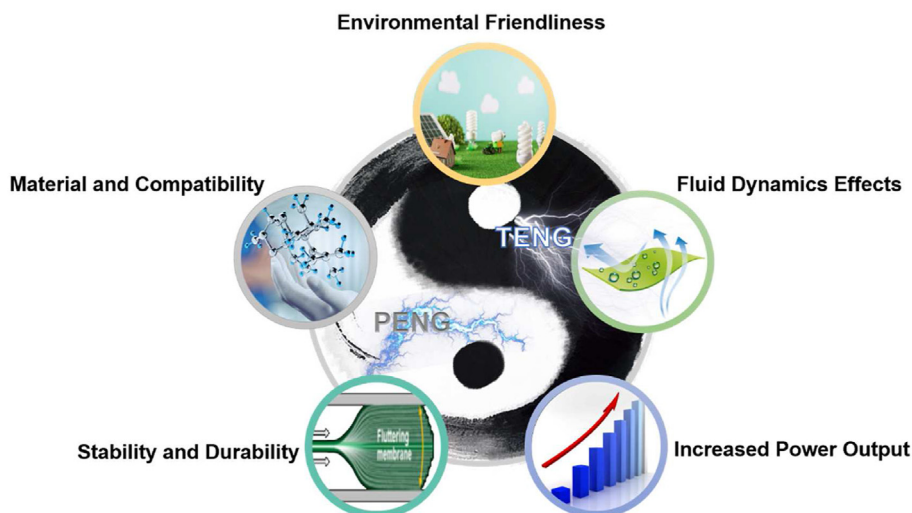


Fig. 17. Challenges and future perspectives.

challenge posed by flow-induced vibrations and their environmental impact. Flow-induced vibrations may subject these nanogenerators to excessive mechanical stress and strain, leading to material fatigue, microcracks, and ultimately, device failure. This not only impacts the efficiency and lifespan of the devices but could also have potential environmental consequences due to material degradation. Particularly in the deployment of these devices in ecologically sensitive areas, it is important to consider their impact on local ecosystems, which might include alterations in wildlife behavior and disturbances to natural habitats. Additionally, the degradation of these devices under environmental stress could result in the dispersal of harmful materials, thereby posing long-term environmental risks, including soil and water contamination. Therefore, it is imperative to emphasize the importance of conducting comprehensive environmental impact assessments (EIAs) prior to the large-scale deployment of these technologies. We recommend the use of environmentally friendly materials, designing devices with enhanced durability, and undertaking comprehensive environmental impact studies to reduce the environmental footprint of these technologies.

Utilizing TENGs and PENGs for flow-induced vibration energy collection presents several pivotal considerations that underscore the complexity and challenges involved. First, the selection of materials is of paramount importance, necessitating their corrosion resistance and triboelectric/piezoelectric performance within fluid environments to ensure consistent operation. Additionally, fluid dynamics exert an influence on the interaction between nanogenerators and flowing fluid, subsequently affecting charge generation efficiency. Addressing this challenge involves optimizing structure design to mitigate these influences, which proves to be a demanding task. Another significant facet concerns efficiency and power output, given that the motion induced by flow-generated vibrations commonly manifests as low-frequency and low-amplitude phenomena. This could influence the energy conversion efficiency and power output of nanogenerators. Conquering the challenge involves ensuring consistent and ample energy conversion across diverse flow conditions. Simultaneously, extended exposure to fluid environments, particularly within hostile or corrosive settings, could initiate device degradation, subsequently affecting the long-term stability and durability of the equipment. Last, incorporating TENGs and PENGs into fluid flow systems necessitates addressing concerns of environmental friendliness and mechanical compatibility. This involves ensuring that the integration does not disrupt fluid flow characteristics while concurrently preventing the introduction of extra resistance. In summary, employing TENGs and PENGs for flow-induced vibration energy collection is a complex endeavor that necessitates comprehensive consideration of multifaceted factors, encompassing materials, dynamics, efficiency, stability, and environmental compatibility, among numerous challenges.

6.2. Corresponding solution

A series of innovative solutions can be devised to tackle the diverse challenges presented above to the applications of TENGs and PENGs in flow-induced vibrations. This can involve the integration of materials science, engineering design and system optimization to realize the efficient utilization of these energy harvesting technologies. The following will provide an overview of potential solutions for each challenge.

6.2.1. Material selection and compatibility

For TENGs and PENGs, exploring the development of materials with strong durability and stability to adapt to fluid environments is crucial. This could involve material surface coatings, protective

materials, or material composites to enhance corrosion resistance and durability. For TENGs, considering materials that generate more controllable charges during interaction with fluids can be beneficial. Additionally, nanomaterial engineering can be utilized to adjust material friction characteristics and charge generation capabilities.

6.2.2. Impact of fluid dynamics

To counteract the influence of fluid dynamics on the performance of TENGs and PENGs, minimizing this effect can be achieved through optimized design and fluid dynamics simulations. Adjusting the shape, size, and structure of TENGs and PENGs can reduce the interference of fluids with the devices. Additionally, utilizing numerical simulations and experimental validation can provide in-depth insights into variations in charge generation efficiency under different fluid conditions, thereby optimizing device performance.

6.2.3. Enhancement of efficiency and power output

For TENGs, designing multistage or multilayer structures can lead to higher charge generation efficiency and energy conversion efficiency. Leveraging mechanical amplification effects to convert small mechanical movements into larger deformations can increase charge generation. For PENGs, considering multidimensional structures can enable the utilization of energy from multiple mechanical motion directions. Furthermore, the role of magnets in enhancing output performance should be noted. For instance, magnets can be integrated into TENGs to produce more consistent and controllable mechanical motion, which is crucial for generating triboelectric charges. By leveraging magnetic fields, the relative motion between different parts of the TENGs can be better regulated, thereby more effectively generating charges. Additionally, magnets can be utilized to induce resonance within TENGs, further amplifying the mechanical movement and thereby enhancing the output power. In PENGs, magnets can also be used to apply a consistent and tunable mechanical force, thus enhancing the deformation of piezoelectric materials. Such a consistent force can lead to a more uniform and optimized strain distribution within the piezoelectric material, thereby improving energy conversion efficiency.

6.2.4. Stability and durability

In the design of TENGs and PENGs, the selection of robust materials and coatings is essential to counteract degradation and corrosion caused by fluid environments. Furthermore, implementing dust-proof, waterproof, and anticorrosion measures is crucial to ensure the long-term stability of these devices under adverse conditions. Special attention should be given to materials capable of withstanding high humidity, temperature fluctuations, salt spray corrosion, and other chemical and physical attacks that may arise from fluid environments. Additionally, structural measures should be taken to enhance the durability of TENGs and PENGs. For example, optimizing the structural design of the devices can reduce material fatigue caused by prolonged vibrations or repetitive stress. Moreover, adopting a modular design allows for the easy replacement of damaged parts without the need for a complete overhaul, thereby not only improving the maintainability of the devices but also reducing the long-term operational costs.

6.2.5. Mechanical compatibility and environmental adaptability

To ensure seamless integration of TENGs and PENGs with fluid systems, frictionless integration can be achieved through meticulously designed structures and interfaces. Utilizing flexible materials and adjustable connectors can mitigate the impact on fluid flow. Additionally, the implementation of intelligent control

systems can minimize noise and various adverse environmental effects. In summary, various comprehensive solutions can be employed to address the challenges faced by TENGs and PENGs in fluid-induced vibrations. These encompass materials selection, design optimization, intelligent control, and system integration, among other aspects. Through interdisciplinary collaboration and continuous research efforts, these challenges can be overcome, enabling the effective application of these energy harvesting technologies in fluid environments. These solutions will contribute to advancing the development of sustainable energy collection and utilization, offering innovative solutions for future energy demands.

6.3. Normalization of performance parameters

When exploring the application of energy harvesting technologies in fluid environments, comparing and studying the performance of different techniques is an important and challenging task. To ensure accurate assessment of the relative performance of different technologies in various application scenarios, the normalization of performance parameters is particularly crucial. This process eliminates the influence of factors like units and dimensions, making the comparison results more reliable and comparable. Normalization methods include aspects such as comparing by unit area or unit volume, energy density, energy conversion efficiency, frequency response, and stability. Comparing by unit area or unit volume allows us to associate energy output with device size, enabling a fair comparison of devices of different sizes. The energy density standardizes energy output to unit volume or mass, aiding in evaluating the energy harvesting capability of different technologies. The energy conversion efficiency reflects the efficiency of converting mechanical energy into electrical energy, serving as a crucial indicator for evaluating energy conversion efficiency. Normalized comparison of frequency response involves standardizing the performance of different technologies within specific frequency ranges, enabling us to understand their performance within the vibration frequency range. Comparisons related to stability and lifespan can combine a device's lifespan with its performance, yielding a normalized indicator of stability. To ensure the accuracy of comparisons, selecting appropriate reference values and normalization methods is crucial. Therefore, we call for future research to adopt uniform normalization methods to maintain consistency in the performance assessment of various energy harvesting technologies. This will facilitate more comprehensive and accurate comparisons and evaluations, providing a more reliable foundation for further research and practical applications.

7. Conclusion

In recent years, the field of nanogenerators utilizing fluid-induced vibration has undergone rapid development, bringing forth new prospects for energy harvesting and sustainable development. Through in-depth research on PENGs and TENGs, our understanding of fluid dynamics and charge separation mechanisms has been deepened. This article systematically explores the core aspects of this field, starting from the theoretical foundations of PENGs and TENGs and extending to the applications of different types of nanogenerators in fluid-induced vibration. In flow-induced vibration phenomenon, we have observed the utilization of various mechanisms, including vortex-induced vibration (VIV), galloping, fluttering, and wake-induced vibration, enriching the energy conversion efficiency and application scope of PENGs and TENGs. However, despite making significant progress, nanogenerators still face challenges in utilizing fluid-induced vibrations. One of these challenges is the normalization of performance parameters, as

different types of generators often use distinct performance parameters to measure their efficiency, which limits direct comparisons among different generators. In addition, the material stability and sustainability are also noteworthy concerns, with the long-term stability of nanogenerators being crucial for their practical feasibility. To overcome these challenges, the interdisciplinary collaboration is essential. Integrating expertise from fields such as material science, fluid dynamics, and electronic engineering can help address the current issues. Importantly, close collaboration with the industry will facilitate the innovative application of these nanogenerators in practical engineering, promoting their commercialization and market adoption. Looking ahead, with the continuous advancement of materials science and nanotechnology, nanogenerators utilizing fluid-induced vibration will play a more significant role in energy harvesting and sustainable development.

Statement

During the preparation of this work the author used ChatGPT4 in order to improve language quality. After using this tool, the author reviewed and edited the content as needed and take full responsibility for the content of the publication.

CRediT authorship contribution statement

Mengwei Wu: Writing – original draft, Visualization, Investigation, Conceptualization. **Chuanqing Zhu:** Investigation, Data curation. **Xiangtao Liu:** Investigation. **Hao Wang:** Writing – review & editing, Resources. **Jicang Si:** Writing – review & editing. **Minyi Xu:** Writing – review & editing, Resources, Funding acquisition. **Jianchun Mi:** Writing – review & editing, Supervision, Funding acquisition.

Declaration of competing interest

The authors declare that they have no known competing financial interests or personal relationships that could have appeared to influence the work reported in this paper.

Data availability

Data will be made available on request.

Acknowledgments

The financial support of National Natural Science Foundation of China (Grant No. 11972048, 52101382, 52371345), the National Key R & D Project from Minister of Science and Technology (2021YFA1201604), the China Scholarship Council (CSC) under the Grant CSC No. 202206010146; 202306570038, are gratefully acknowledged.

References

- [1] B. Reeder, A. David, Health at hand: a systematic review of smart watch uses for health and wellness, *J. Biomed. Inf.* 63 (2016) 269–276, <https://doi.org/10.1016/j.jbi.2016.09.001>.
- [2] D.J. Wile, R. Ranawaya, Z.H. Kiss, Smart watch accelerometry for analysis and diagnosis of tremor, *J. Neurosci. Methods* 230 (2014) 1–4, <https://doi.org/10.1016/j.jneumeth.2014.04.021>.
- [3] F. A, Exploring the adoption of smartphone technology: literature review, in: *Proceedings of PICMET'12: Technology Management for Emerging Technologies*, 2012, pp. 2758–2770, <https://doi.org/10.1109/picmet.2015.7273210>, 2012.
- [4] M. Soori, B. Arezoo, R. Dastres, Internet of things for smart factories in industry 4.0, a review, *Intern. Things Cyber Phys. Syst.* 3 (2023) 192–204, <https://doi.org/10.1016/j.iotcps.2023.04.006>.

- [5] S. Li, L.D. Xu, S. Zhao, The internet of things: a survey, *Inf. Syst. Front* 17 (2014) 243–259, <https://doi.org/10.1007/s10796-014-9492-7>.
- [6] S. Madakam, R. Ramaswamy, S. Tripathi, Internet of things (IoT): a literature review, *J. Comput. Commun.* 3 (2015) 164–173.
- [7] A.G. Olabi, T. Wilberforce, E.T. Sayed, A.G. Abo-Khalil, H.M. Maghrabie, K. Elsaid, et al., Battery energy storage systems and SWOT (strengths, weaknesses, opportunities, and threats) analysis of batteries in power transmission, *Energy* 254 (2022) 123987, <https://doi.org/10.1016/j.energy.2022.123987>.
- [8] D. Patil, M.K. McDonough, J.M. Miller, B. Fahimi, P.T. Balsara, Wireless power transfer for vehicular applications: overview and challenges, *IEEE Trans. Transport. Electrif.* 4 (2018) 3–37, <https://doi.org/10.1109/tte.2017.2780627>.
- [9] Z. Zhang, H. Pang, A. Georgiadis, C. Cecati, Wireless power transfer—an overview, *IEEE Trans. Ind. Electron.* 66 (2019) 1044–1058.
- [10] J. Huang, Y. Zhou, Z. Ning, H. Gharavi, Wireless power transfer and energy harvesting: current status and future prospects, *IEEE Wireless Commun.* 26 (2019) 163–169, <https://doi.org/10.1109/mwc.2019.1800378>.
- [11] M. Kazemi, H. Zareipour, Long-term scheduling of battery storage systems in energy and regulation markets considering battery's lifespan, *IEEE Trans. Smart Grid* 9 (2018) 6840–6849, <https://doi.org/10.1109/tsg.2017.2724919>.
- [12] K.K. Duru, C. Karra, P. Venkatachalam, S.A. Betha, A. Anish Madhavan, S. Kalluri, Critical insights into Fast charging techniques for lithium-ion batteries in electric vehicles, *IEEE Trans. Device Mater. Reliab.* 21 (2021) 137–152, <https://doi.org/10.1109/tdmr.2021.3051840>.
- [13] M.A. Hannan, M.S.H. Lipu, A. Hussain, A. Mohamed, A review of lithium-ion battery state of charge estimation and management system in electric vehicle applications: challenges and recommendations, *Renew. Sustain. Energy Rev.* 78 (2017) 834–854, <https://doi.org/10.1016/j.rser.2017.05.001>.
- [14] G.M. Joselin Herbert, S. Iniyar, E. Sreevalsan, S. Rajapandian, A review of wind energy technologies, *Renew. Sustain. Energy Rev.* 11 (2007) 1117–1145.
- [15] A. Sahin, Progress and recent trends in wind energy, *Prog. Energy Combust. Sci.* 30 (2004) 501–543.
- [16] D. Kamani, M.M. Ardehali, Long-term forecast of electrical energy consumption with considerations for solar and wind energy sources, *Energy* 268 (2023) 126617, <https://doi.org/10.1016/j.energy.2023.126617>.
- [17] K. Govindan, Pathways to low carbon energy transition through multi criteria assessment of offshore wind energy barriers, *Technol. Forecast. Soc. Change* 187 (2023) 122131, <https://doi.org/10.1016/j.techfore.2022.122131>.
- [18] C. Wei, X. Jing, A comprehensive review on vibration energy harvesting: modelling and realization, *Renew. Sustain. Energy Rev.* 74 (2017) 1–18, <https://doi.org/10.1016/j.rser.2017.01.073>.
- [19] X. Ma, S. Zhou, A review of flow-induced vibration energy harvesters, *Energy Convers. Manag.* 254 (2022) 115223, <https://doi.org/10.1016/j.enconman.2022.115223>.
- [20] A. Mohanty, S. Parida, R.K. Behera, T. Roy, Vibration energy harvesting: a review, *J. Adv. Dielect.* 9 (2019) 1930001.
- [21] S.L.M. Zhou, A. Erturk, Multistable vibration energy harvesters: principle, progress, and perspectives, *J. Sound Vib.* 528 (2022) 116886.
- [22] M.A.A. Abdelkareem, L. Xu, M.K.A. Ali, A. Elagouz, J. Mi, S. Guo, et al., Vibration energy harvesting in automotive suspension system: a detailed review, *Appl. Energy* 229 (2018) 672–699, <https://doi.org/10.1016/j.jsv.2022.116886>.
- [23] G. Sui, X. Shan, C. Hou, H. Tian, J. Hu, T. Xie, An underwater piezoelectric energy harvester based on magnetic coupling adaptable to low-speed water flow, *Mech. Syst. Signal Process.* 184 (2023) 109729, <https://doi.org/10.1016/j.ymssp.2022.109729>.
- [24] M. Hafizh, A.G.A. Muthalif, J. Renno, M.R. Paurobally, M.S. Mohamed Ali, A vortex-induced vibration-based self-tunable airfoil-shaped piezoelectric energy harvester for remote sensing applications in water, *Ocean Eng.* 269 (2023) 113467, <https://doi.org/10.1016/j.oceaneng.2022.113467>.
- [25] C. Song, X. Zhu, M. Wang, P. Yang, L. Chen, L. Hong, et al., Recent advances in ocean energy harvesting based on triboelectric nanogenerators, *Sustain. Energy Technol. Assessments* 53 (2022) 102767, <https://doi.org/10.1016/j.seta.2022.102767>.
- [26] P. Munirathinam, A. Anna Mathew, V. Shanmugasundaram, V. Vivekananthan, Y. Purusothaman, S.-J. Kim, et al., A comprehensive review on triboelectric nanogenerators based on Real-Time applications in energy harvesting and Self-Powered sensing, *Mater. Sci. Eng. B* 297 (2023) 116762, <https://doi.org/10.1016/j.mseb.2023.116762>.
- [27] Z.L. Wang, T. Jiang, L. Xu, Toward the blue energy dream by triboelectric nanogenerator networks, *Nano Energy* 39 (2017) 9–23, <https://doi.org/10.1016/j.nanoen.2017.06.035>.
- [28] Z.L. Wang, Triboelectric nanogenerator (TENG)—sparking an energy and sensor revolution, *Adv. Energy Mater.* 10 (2020) 2000137, <https://doi.org/10.1002/aenm.202000137>.
- [29] N. Sezer, M. Koç, A comprehensive review on the state-of-the-art of piezoelectric energy harvesting, *Nano Energy* 80 (2021) 105567, <https://doi.org/10.1016/j.nanoen.2020.105567>.
- [30] X. Zheng, L. He, S. Wang, X. Liu, R. Liu, G. Cheng, A review of piezoelectric energy harvesters for harvesting wind energy, *Sens. Actuators A Phys.* 352 (2023) 114190, <https://doi.org/10.1016/j.sna.2023.114190>.
- [31] J.L. Birman, Theory of the piezoelectric effect in the zincblende structure, *Phys. Rev.* 111 (1958) 1510–1514, <https://doi.org/10.1103/physrev.111.1510>.
- [32] M.H.L.L.S. Shamos, M.I. Shamos, Piezoelectric effect in bone, *Nature* 197 (1963) 81, <https://doi.org/10.1038/197081a0>.
- [33] R.S.L.A. Theissmann, J. Kling, et al., Nanodomains in morphotropic PZT ceramics: on the origin of the strong piezoelectric effect, *J. Appl. Phys.* 102 (2007) 024111, <https://doi.org/10.1063/1.2753569>.
- [34] S.K. Kim, R. Bhatia, T.-H. Kim, D. Seol, J.H. Kim, H. Kim, et al., Directional dependent piezoelectric effect in CVD grown monolayer MoS₂ for flexible piezoelectric nanogenerators, *Nano Energy* 22 (2016) 483–489, <https://doi.org/10.1016/j.nanoen.2016.02.046>.
- [35] H. Jaffe, Piezoelectric ceramics, *J. Am. Ceram. Soc.* 41 (1958) 494–498.
- [36] K.H. Michel, B. Verberck, Theory of elastic and piezoelectric effects in two-dimensional hexagonal boron nitride, *Phys. Rev. B* 80 (2009) 224301, <https://doi.org/10.1103/physrevb.80.224301>.
- [37] S. Pan, Z. Zhang, Fundamental theories and basic principles of triboelectric effect: a review, *Friction* 7 (2018) 2–17, <https://doi.org/10.1007/s40544-018-0217-7>.
- [38] S. Niu, Z.L. Wang, Theoretical systems of triboelectric nanogenerators, *Nano Energy* 14 (2015) 161–192, <https://doi.org/10.1016/j.nanoen.2014.11.034>.
- [39] L. Zhou, D. Liu, J. Wang, Z.L. Wang, Triboelectric nanogenerators: fundamental physics and potential applications, *Friction* 8 (2020) 481–506, <https://doi.org/10.1007/s40544-020-0390-3>.
- [40] Y. Wang, Y. Yang, Z.L. Wang, Triboelectric nanogenerators as flexible power sources, *NPJ Flex. Electron.* 1 (2017) 1–10, <https://doi.org/10.1038/s41528-017-0007-8>.
- [41] L. WZ, Triboelectric nanogenerators as new energy technology for self-powered systems and as active mechanical and chemical sensors, *ACS Nano* 7 (2013) 9533–9557, <https://doi.org/10.1021/nn404614z>.
- [42] J. Wang, D. Yurchenko, G. Hu, L. Zhao, L. Tang, Y. Yang, Perspectives in flow-induced vibration energy harvesting, *Appl. Phys. Lett.* 119 (2021) 100502, <https://doi.org/10.1063/5.0063488>.
- [43] D. Z. Vibration energy harvesting: machinery vibration, human movement and flow induced vibration, *Sustain. Energy Harvest. Technol. Past, Present Future* 1 (2011) 22–54, <https://doi.org/10.5772/25731>.
- [44] D.A. Wang, H.H. Ko, Piezoelectric energy harvesting from flow-induced vibration, *J. Micromech. Microeng.* 20 (2010) 025019, <https://doi.org/10.1088/0960-1317/20/2/025019>.
- [45] X. Shan, H. Li, Y. Yang, J. Feng, Y. Wang, T. Xie, Enhancing the performance of an underwater piezoelectric energy harvester based on flow-induced vibration, *Energy* 172 (2019) 134–140, <https://doi.org/10.1016/j.energy.2019.01.120>.
- [46] H. Zhu, T. Tang, H. Yang, J. Wang, J. Song, G. Peng, et al., The state-of-the-art brief review on piezoelectric energy harvesting from flow-induced vibration, *Shock Vib.* 2021 (2021) 1–19, <https://doi.org/10.1155/2021/8861821>.
- [47] X. Fan, Z. Wang, X. Chen, Y. Wang, W. Tan, Experimental investigation on flow-induced vibration of flexible multi cylinders in atmospheric boundary layer, *Int. J. Mech. Sci.* (2020) 183, <https://doi.org/10.1016/j.ijmeccsci.2020.105815>.
- [48] T. Tang, H. Zhu, J. Song, B. Ma, T. Zhou, The state-of-the-art review on the wake alteration of a rotating cylinder and the associated interaction with flow-induced vibration, *Ocean Eng.* 254 (2022) 111340, <https://doi.org/10.1016/j.oceaneng.2022.111340>.
- [49] A. Leonard, A. Roshko, Aspects of flow-induced vibration, *J. Fluid Struct.* 15 (2001) 415–425, <https://doi.org/10.1006/jfls.2000.0360>.
- [50] J. Wang, L. Sheng, L. Ding, A comprehensive numerical study on flow-induced vibrations with various groove structures: suppression or enhancing energy scavenging, *Ocean Eng.* 271 (2023) 113781, <https://doi.org/10.1016/j.oceaneng.2023.113781>.
- [51] J. Li, Y. Long, F. Yang, X. Wang, Respiration-driven triboelectric nanogenerators for biomedical applications, *EcoMat* 2 (2020) e12045, <https://doi.org/10.1002/eom.2.12045>.
- [52] Y. Su, G. Chen, C. Chen, Q. Gong, G. Xie, M. Yao, et al., Self-powered respiration monitoring enabled by a triboelectric nanogenerator, *Adv. Mater.* 33 (2021) e2101262.
- [53] P. Škvorc, H. Kozmar, Wind energy harnessing on tall buildings in urban environments, *Renew. Sustain. Energy Rev.* 152 (2021) 111662, <https://doi.org/10.1016/j.rser.2021.111662>.
- [54] E. Dayan, Wind energy in buildings, *Refocus* 7 (2006) 33–38.
- [55] H. Zhou, Y. Lu, X. Liu, R. Chang, B. Wang, Harvesting wind energy in low-rise residential buildings: design and optimization of building forms, *J. Clean. Prod.* 167 (2017) 306–316, <https://doi.org/10.1016/j.jclepro.2017.08.166>.
- [56] C. Zhu, M. Wu, C. Liu, C. Xiang, R. Xu, H. Yang, et al., Highly integrated triboelectric-electromagnetic wave energy harvester toward self-powered marine Buoy, *Adv. Energy Mater.* (2023) 2301665, <https://doi.org/10.1002/aenm.202301665>.
- [57] F. Shen, Z. Li, H. Guo, Z. Yang, H. Wu, M. Wang, et al., Recent advances towards ocean energy harvesting and self-powered applications based on triboelectric nanogenerators, *Adv. Electron. Mater.* 7 (2021) 2100277, <https://doi.org/10.1002/aelm.202100277>.
- [58] S. Panda, S. Hajra, Y. Oh, W. Oh, J. Lee, H. Shin, et al., Hybrid nanogenerators for ocean energy harvesting: mechanisms, designs, and applications, *Small* 19 (2023) e2300847, <https://doi.org/10.1002/sml.202300847>.
- [59] T. Zhao, M. Xu, X. Xiao, Y. Ma, Z. Li, Z.L. Wang, Recent progress in blue energy harvesting for powering distributed sensors in ocean, *Nano Energy* 88 (2021) 106199, <https://doi.org/10.1016/j.nanoen.2021.106199>.

- [60] N.V. Viet, X.D. Xie, K.M. Liew, N. Banthia, Q. Wang, Energy harvesting from ocean waves by a floating energy harvester, *Energy*, 112 (2016) 1219–1226, <https://doi.org/10.1016/j.energy.2016.07.019>.
- [61] N. Wu, Q. Wang, X. Xie, Ocean wave energy harvesting with a piezoelectric coupled buoy structure, *Appl. Ocean Res.* 50 (2015) 110–118, <https://doi.org/10.1016/j.apor.2015.01.004>.
- [62] C. Rodrigues, D. Nunes, D. Clemente, N. Mathias, J.M. Correia, P. Rosa-Santos, et al., Emerging triboelectric nanogenerators for ocean wave energy harvesting: state of the art and future perspectives, *Energy Environ. Sci.* 13 (2020) 2657–2683, <https://doi.org/10.1039/d0ee01258k>.
- [63] S.M. Hasheminejad, Y. Masoumi, Dual-functional synergetic energy harvesting and flow-induced vibration control of an electromagnetic-based square cylinder integrated with a flexible bimorph piezoelectric wake splitter plate, *Renew. Energy* 216 (2023) 119133, <https://doi.org/10.2139/ssrn.4325656>.
- [64] S. Salem, K. Fraña, Harvesting energy of flow-induced vibrations using cylindrical piezoelectric transducers, *Energy Rep.* 9 (2023) 279–285, <https://doi.org/10.1016/j.egy.2022.12.113>.
- [65] M. Hafizh, A.G.A. Muthalif, J. Renno, M.R. Paurobally, I. Bahadur, H. Ouakad, et al., Vortex induced vibration energy harvesting using magnetically coupled broadband circular-array piezoelectric patch: modelling, parametric study, and experiments, *Energy Convers. Manag.* 276 (2023) 116559, <https://doi.org/10.1016/j.enconman.2022.116559>.
- [66] B. Lin, Y. Wang, Y. Qian, Bursting oscillation and its mechanism of the flow-induced vibration piezoelectric energy harvester with magnets by low-frequency excitation, *Eur. Phys. J. Spec. Top.* 231 (2022) 2237–2248, <https://doi.org/10.1140/epjs/s11734-022-00481-1>.
- [67] M. Mariello, F. Guido, V.M. Mastronardi, M.T. Todaro, D. Desmaële, M. De Vittorio, Nanogenerators for harvesting mechanical energy conveyed by liquids, *Nano Energy*, 57 (2019) 141–156, <https://doi.org/10.1016/j.nanoen.2018.12.027>.
- [68] H. Deng, J. Ye, Y. Du, J. Zhang, M. Ma, X. Zhong, Bistable broadband hybrid generator for ultralow-frequency rectilinear motion, *Nano Energy*, 65 (2019) 103973, <https://doi.org/10.1016/j.nanoen.2019.103973>.
- [69] A. Abdelkefi, J.M. Scanlon, E. McDowell, M.R. Hajj, Performance enhancement of piezoelectric energy harvesters from wake galloping, *Appl. Phys. Lett.* 103 (2013) 033903, <https://doi.org/10.1063/1.4816075>.
- [70] Y. Yang, L. Zhao, L. Tang, Comparative study of tip cross-sections for efficient galloping energy harvesting, *Appl. Phys. Lett.* 102 (2013) 064105, <https://doi.org/10.1063/1.4792737>.
- [71] B. Shi, Q. Wang, H. Su, J. Li, B. Xie, P. Wang, et al., Progress in recent research on the design and use of triboelectric nanogenerators for harvesting wind energy, *Nano Energy*, (2023) 108789, <https://doi.org/10.1016/j.nanoen.2023.108789>.
- [72] J. Wang, L. Geng, L. Ding, H. Zhu, D. Yurchenko, The state-of-the-art review on energy harvesting from flow-induced vibrations, *Appl. Energy* 267 (2020) 114902, <https://doi.org/10.1016/j.apenergy.2020.114902>.
- [73] Q. Xia, N. Song, C. Liu, R. Zhai, C. Ai, X. Sun, et al., Current development of bionic flexible sensors applied to marine flow field detection, *Sens. Actuat. A Phys.* 351 (2023) 114158, <https://doi.org/10.1016/j.sna.2023.114158>.
- [74] J. Wang, G. Li, M. Zhang, G. Zhao, Z. Jin, K. Xu, et al., Energy harvesting from flow-induced vibration: a lumped parameter model, *Energy Sourc. Part A Recovery, Util. Environ. Eff.* 40 (2018) 2903–2913, <https://doi.org/10.1080/15567036.2018.1513100>.
- [75] S. Oveissi, M. Salehi, A. Ghassemi, S. Ali Eftekhari, S. Ziaei-Rad, Energy harvesting of nanofluid-conveying axially moving cylindrical composite nanoshells of integrated CNT and piezoelectric layers with magnetorheological elastomer core under external fluid vortex-induced vibration, *J. Magn. Magn Mater.* 572 (2023) 170551, <https://doi.org/10.1016/j.jmmm.2023.170551>.
- [76] G. Sui, X. Shan, H. Tian, L. Wang, T. Xie, Study on different underwater energy harvester arrays based on flow-induced vibration, *Mech. Syst. Signal Process.* 167 (2022) 108546, <https://doi.org/10.1016/j.ymssp.2021.108546>.
- [77] P. Han, G. Pan, B. Zhang, W. Wang, W. Tian, Three-cylinder oscillator under flow: flow induced vibration and energy harvesting, *Ocean Eng.* 211 (2020) 107619, <https://doi.org/10.1016/j.oceaneng.2020.107619>.
- [78] Y. Gong, X. Shan, X. Luo, J. Pan, T. Xie, Z. Yang, Direction-adaptive energy harvesting with a guide wing under flow-induced oscillations, *Energy* 187 (2019) 115983, <https://doi.org/10.1016/j.energy.2019.115983>.
- [79] V. Tamimi, J. Wu, M.J. Esfehiani, M. Zeinoddini, S.T.O. Naeeni, Comparison of hydrokinetic energy harvesting performance of a fluttering hydrofoil against other Flow-Induced Vibration (FIV) mechanisms, *Renew. Energy* 186 (2022) 157–172, <https://doi.org/10.1016/j.renene.2021.12.127>.
- [80] J. Wang, C. Zhang, M. Zhang, A. Abdelkefi, H. Yu, X. Ge, et al., Enhancing energy harvesting from flow-induced vibrations of a circular cylinder using a downstream rectangular plate: an experimental study, *Int. J. Mech. Sci.* 211 (2021) 106781, <https://doi.org/10.1016/j.ijmecsci.2021.106781>.
- [81] Y. Feng, J. Hu, S. Afshan, M. Irfan, M. Hu, S. Abbas, Bridging resource disparities for sustainable development: a comparative analysis of resource-rich and resource-scarce countries, *Resour. Pol.* 85 (2023) 103981, <https://doi.org/10.1016/j.resourpol.2023.103981>.
- [82] Q. Zhang, C. Prouty, J.B. Zimmerman, J.R. Mihelcic, More than target 6.3: a systems approach to rethinking sustainable development goals in a resource-scarce world, *Engineering* 2 (2016) 481–489, <https://doi.org/10.1016/j.eng.2016.04.010>.
- [83] H. Li, J. Wen, Z. Ou, et al., Leaf-like TENGs for harvesting gentle wind energy at an air velocity as low as 0.2 ms⁻¹, *Adv. Funct. Mater.* 33 (2023) 2212207, <https://doi.org/10.1002/adfm.202212207>.
- [84] R.E.H. Sims, H.-H. Rogner, K. Gregory, Carbon emission and mitigation cost comparisons between fossil fuel, nuclear and renewable energy resources for electricity generation, *Energy Pol.* 31 (2003) 1315–1326, [https://doi.org/10.1016/s0301-4215\(02\)00192-1](https://doi.org/10.1016/s0301-4215(02)00192-1).
- [85] Z. Liu, D. Guan, W. Wei, S.J. Davis, P. Ciais, J. Bai, et al., Reduced carbon emission estimates from fossil fuel combustion and cement production in China, *Nature* 524 (2015) 335–338, <https://doi.org/10.1038/nature14677>.
- [86] I. Hanif, Impact of fossil fuels energy consumption, energy policies, and urban sprawl on carbon emissions in East Asia and the Pacific: a panel investigation, *Energy Strategy Rev.* 21 (2018) 16–24, <https://doi.org/10.1016/j.esr.2018.04.006>.
- [87] J. Hansen, P. Kharecha, M. Sato, V. Masson-Delmotte, F. Ackerman, D.J. Beerling, et al., Assessing "dangerous climate change": required reduction of carbon emissions to protect young people, future generations and nature, *PLoS One*, 8 (2013) e81648, <https://doi.org/10.1201/9781315365633-23>.
- [88] D. Cao, X. Ding, X. Guo, M. Yao, Design, simulation and experiment for a vortex-induced vibration energy harvester for low-velocity water flow, *Int. J. Precis. Eng. Manuf. Green Technol.* 8 (2020) 1239–1252.
- [89] U. Javed, A. Abdelkefi, Characteristics and comparative analysis of piezoelectric-electromagnetic energy harvesters from vortex-induced oscillations, *Nonlinear Dynam.* 95 (2019) 3309–3333, <https://doi.org/10.1007/s11071-018-04757-x>.
- [90] S. Adhikari, A. Rastogi, B. Bhattacharya, Piezoelectric vortex induced vibration energy harvesting in a random flow field, *Smart Mater. Struct.* 29 (2020) 035034, <https://doi.org/10.1088/1361-665x/ab519f>.
- [91] I. Mehdipour, F. Madaro, F. Rizzi, M. De Vittorio, Comprehensive experimental study on bluff body shapes for vortex-induced vibration piezoelectric energy harvesting mechanisms, *Energy Convers. Manag.* X 13 (2022) 100174, <https://doi.org/10.1016/j.ecmx.2021.100174>.
- [92] Z. Ren, L. Wu, Y. Pang, W. Zhang, R. Yang, Strategies for effectively harvesting wind energy based on triboelectric nanogenerators, *Nano Energy*, 100 (2022) 107522, <https://doi.org/10.1016/j.nanoen.2022.107522>.
- [93] S.M.X. Wang, X. Wang, Elasto-aerodynamics-driven triboelectric nanogenerator for scavenging air-flow energy, *ACS Nano*, 9 (2015) 9554–9563, <https://doi.org/10.1021/acsnano.5b04396>.
- [94] Z. Ren, Z. Wang, F. Wang, S. Li, Z.L. Wang, Vibration behavior and excitation mechanism of ultra-stretchable triboelectric nanogenerator for wind energy harvesting, *Extreme Mech. Lett.* 45 (2021) 101285, <https://doi.org/10.1016/j.eml.2021.101285>.
- [95] Q.-T. Nguyen, K.-K.K. Ahn, Fluid-based triboelectric nanogenerators: a review of current status and applications, *Int. J. Precis. Eng. Manuf. Green Technol.* 8 (2020) 1043–1060, <https://doi.org/10.1007/s40684-020-00255-x>.
- [96] A. Matin Nazar, Y. Narazaki, A. Rayegani, F. Rahimi Sardo, Recent progress of triboelectric nanogenerators as self-powered sensors in transportation engineering, *Measurement* 203 (2022) 112010, <https://doi.org/10.1016/j.measurement.2022.112010>.
- [97] M. Zhang, C. Zhang, A. Abdelkefi, H. Yu, O. Gaidai, X. Qin, et al., Piezoelectric energy harvesting from vortex-induced vibration of a circular cylinder: effect of Reynolds number, *Ocean Eng.* 235 (2021) 109378, <https://doi.org/10.1016/j.oceaneng.2021.109378>.
- [98] A. Bibo, M.F. Daqaq, On the optimal performance and universal design curves of galloping energy harvesters, *Appl. Phys. Lett.* 104 (2014) 023901, <https://doi.org/10.1063/1.4861599>.
- [99] H. Elahi, M. Eugeni, F. Fune, L. Lampani, F. Mastroddi, G. Paolo Romano, et al., Performance evaluation of a piezoelectric energy harvester based on flag-flutter, *Micromachines* 11 (2020) 933, <https://doi.org/10.3390/mi11100933>.
- [100] Z. Li, S. Zhou, Z. Yang, Recent progress on flutter-based wind energy harvesting, *Int. J. Manuf. Syst. Des.* 2 (2022) 82–98, <https://doi.org/10.1002/msd2.12035>.
- [101] A.H. Alhadidi, M.F. Daqaq, A broadband bi-stable flow energy harvester based on the wake-galloping phenomenon, *Appl. Phys. Lett.* 109 (2016) 033904, <https://doi.org/10.1063/1.4959181>.
- [102] J.S. Kim, J. Kim, J.N. Kim, J. Ahn, J.H. Jeong, I. Park, et al., Collectively exhaustive hybrid triboelectric nanogenerator based on flow-induced impacting-sliding cylinder for ocean energy harvesting, *Adv. Energy Mater.* 12 (2021) 2103076, <https://doi.org/10.1002/aenm.202103076>.
- [103] L. Zhang, B. Meng, Y. Xia, Z. Deng, H. Dai, P. Hagedorn, et al., Galloping triboelectric nanogenerator for energy harvesting under low wind speed, *Nano Energy*, 70 (2020) 104477, <https://doi.org/10.1016/j.nanoen.2020.104477>.
- [104] W. Li, L. Lu, X. Fu, et al., Kármán vortex street driven membrane triboelectric nanogenerator for enhanced ultra-low speed wind energy harvesting and active gas flow sensing, *ACS Appl. Mater. Interfaces* 14 (2022) 51018–51028, <https://doi.org/10.1021/acsaami.2c16350.s005>.
- [105] J. Briscoe, S. Dunn, Piezoelectric nanogenerators – a review of nano-structured piezoelectric energy harvesters, *Nano Energy*, 14 (2015) 15–29, <https://doi.org/10.1016/j.nanoen.2014.11.059>.
- [106] D. Hu, M. Yao, Y. Fan, C. Ma, M. Fan, M. Liu, Strategies to achieve high performance piezoelectric nanogenerators, *Nano Energy*, 55 (2019) 288–304, <https://doi.org/10.1016/j.nanoen.2018.10.053>.

- [107] L. Lu, W. Ding, J. Liu, B. Yang, Flexible PVDF based piezoelectric nanogenerators, *Nano Energy*. 78 (2020) 105251, <https://doi.org/10.1016/j.nanoen.2020.105251>.
- [108] Lin Zhong, J.S. Wang, Piezoelectric nanogenerators based on zinc oxide nanowire arrays, *Science*. 312 (2006) 242–246, <https://doi.org/10.1126/science.1124005>.
- [109] T. Cheng, J. Shao, Z.L. Wang, Triboelectric nanogenerators, *Nat. Rev. Methods Primers* 3 (2023) 39.
- [110] J. Luo, Z.L. Wang, Recent progress of triboelectric nanogenerators: from fundamental theory to practical applications, *EcoMat*. 2 (2020), <https://doi.org/10.1002/eom2.12059>.
- [111] S. Niu, Y. Liu, S. Wang, L. Lin, Y.S. Zhou, Y. Hu, et al., Theory of sliding-mode triboelectric nanogenerators, *Adv. Mater.* 25 (2013) 6184–6193, <https://doi.org/10.1002/adma.201302808>.
- [112] X. Fu, T. Bu, C. Li, G. Liu, C. Zhang, Overview of micro/nano-wind energy harvesters and sensors, *Nanoscale* 12 (2020) 23929–23944, <https://doi.org/10.1039/d0nr06373h>.
- [113] H. Liu, J. Zhong, C. Lee, S.-W. Lee, L. Lin, A comprehensive review on piezoelectric energy harvesting technology: materials, mechanisms, and applications, *Appl. Phys. Rev.* 5 (2018) 041306, <https://doi.org/10.1063/1.5074184>.
- [114] Z.L. Wang, On Maxwell's displacement current for energy and sensors: the origin of nanogenerators, *Mater. Today* 20 (2017) 74–82, <https://doi.org/10.1016/j.mattod.2016.12.001>.
- [115] C. Xu, Y. Zi, A.C. Wang, H. Zou, Y. Dai, X. He, et al., On the electron-transfer mechanism in the contact-electrification effect, *Adv. Mater.* 30 (2018) e1706790, <https://doi.org/10.1002/adma.201706790>.
- [116] Z.L. Wang, On the first principle theory of nanogenerators from Maxwell's equations, *Nano Energy*. 68 (2020) 104272, <https://doi.org/10.1016/j.nanoen.2019.104272>.
- [117] Z.L. Wang, On the expanded Maxwell's equations for moving charged media system – general theory, mathematical solutions and applications in TENG, *Mater. Today* 52 (2022) 348–363, <https://doi.org/10.1016/j.mattod.2021.10.027>.
- [118] C.H.K. Williamson, R. Govardhan, Vortex-induced vibrations, *Annu. Rev. Fluid Mech.* 36 (2004) 413–455.
- [119] L. Cheng, Y. Zhou, M.M. Zhang, Perturbed interaction between vortex shedding and induced vibration, *J. Fluid Struct.* 17 (2003) 887–901, [https://doi.org/10.1016/s0889-9746\(03\)00042-2](https://doi.org/10.1016/s0889-9746(03)00042-2).
- [120] J.R.B.P.W. Meneghini, Numerical simulation of high amplitude oscillatory flow about a circular cylinder, *J. Fluid Struct.* 9 (1995) 435–455, <https://doi.org/10.1006/jfls.1995.1025>.
- [121] H. Li, S. Laima, Q. Zhang, N. Li, Z. Liu, Field monitoring and validation of vortex-induced vibrations of a long-span suspension bridge, *J. Wind Eng. Ind. Aerod.* 124 (2014) 54–67, <https://doi.org/10.1016/j.jweia.2013.11.006>.
- [122] D.W. Carlson, Y. Modarres-Sadeghi, Vortex-induced vibration of spar platforms for floating offshore wind turbines, *Wind Energy*. 21 (2018) 1169–1176, <https://doi.org/10.1002/we.2221>.
- [123] G. Liu, H. Li, Z. Qiu, D. Leng, Z. Li, W. Li, A mini review of recent progress on vortex-induced vibrations of marine risers, *Ocean Eng.* 195 (2020) 106704, <https://doi.org/10.1016/j.oceaneng.2019.106704>.
- [124] D. Li, Y. Wu, A. Da Ronch, X. Xiang, Energy harvesting by means of flow-induced vibrations on aerospace vehicles, *Prog. Aero. Sci.* 86 (2016) 28–62, <https://doi.org/10.1016/j.paerosci.2016.08.001>.
- [125] S.G. Horcas, T. Barlas, F. Zahle, N.N. Sørensen, Vortex induced vibrations of wind turbine blades: influence of the tip geometry, *Phys. Fluids* 32 (2020) 065104, <https://doi.org/10.1063/1.50004005>.
- [126] P. Sidlof, V. Vlček, M. Štěpán, Experimental investigation of flow-induced vibration of a pitch–plunge NACA 0015 airfoil under deep dynamic stall, *J. Fluid Struct.* 67 (2016) 48–59, <https://doi.org/10.1016/j.jfluidstructs.2016.08.011>.
- [127] C. Dongyang, L.K. Abbas, W. Guoping, R. Xiaoting, P. Marzocca, Numerical study of flow-induced vibrations of cylinders under the action of nonlinear energy sinks (NESSs), *Nonlinear Dynam.* 94 (2018) 925–957, <https://doi.org/10.1007/s11071-018-4402-z>.
- [128] L. Song, S. Fu, J. Cao, L. Ma, J. Wu, An investigation into the hydrodynamics of a flexible riser undergoing vortex-induced vibration, *J. Fluid Struct.* 63 (2016) 325–350, <https://doi.org/10.1016/j.jfluidstructs.2016.03.006>.
- [129] Y.J. Lee, Y. Qi, G. Zhou, K.B. Lua, Vortex-induced vibration wind energy harvesting by piezoelectric MEMS device in formation, *Sci. Rep.* 9 (2019) 20404, <https://doi.org/10.1038/s41598-019-56786-0>.
- [130] Z. Deng, L. Xu, H. Qin, X. Li, J. Duan, B. Hou, et al., Rationally structured triboelectric nanogenerator arrays for harvesting water-current energy and self-powered sensing, *Adv. Mater.* 34 (2022) e2205064, <https://doi.org/10.1002/adma.202205064>.
- [131] S. Wang, W. Liao, Z. Zhang, Y. Liao, M. Yan, J. Kan, Development of a novel non-contact piezoelectric wind energy harvester excited by vortex-induced vibration, *Energy Convers. Manag.* 235 (2021) 113980, <https://doi.org/10.1016/j.enconman.2021.113980>.
- [132] X. Fan, K. Guo, Y. Wang, Toward a high performance and strong resilience wind energy harvester assembly utilizing flow-induced vibration: role of hysteresis, *Energy* 251 (2022) 123921, <https://doi.org/10.1016/j.energy.2022.123921>.
- [133] H. Zhu, Y. Gao, Hydrokinetic energy harvesting from flow-induced vibration of a circular cylinder with two symmetrical fin-shaped strips, *Energy* 165 (2018) 1259–1281, <https://doi.org/10.1016/j.energy.2018.10.109>.
- [134] X. Ma, Z. Li, H. Zhang, S. Zhou, Dynamic modeling and analysis of a tristable vortex-induced vibration energy harvester, *Mech. Syst. Signal Process.* 187 (2023) 109924, <https://doi.org/10.1016/j.ymssp.2022.109924>.
- [135] W. Sun, S. Jo, J. Seok, Development of the optimal bluff body for wind energy harvesting using the synergetic effect of coupled vortex induced vibration and galloping phenomena, *Int. J. Mech. Sci.* 156 (2019) 435–445, <https://doi.org/10.1016/j.ijmecsci.2019.04.019>.
- [136] C. Mannini, A.M. Marra, G. Bartoli, VIV–galloping instability of rectangular cylinders: review and new experiments, *J. Wind Eng. Ind. Aerod.* 132 (2014) 109–124.
- [137] Z. Cheng, F.-S. Lien, E.H. Dowell, E. Yee, Triggering of galloping in structures at low Reynolds numbers, *J. Fluid Struct.* 118 (2023) A18, <https://doi.org/10.1016/j.jweia.2014.06.021>.
- [138] F. Duan, Y. Song, S. Gao, Y. Liu, W. Chu, X. Lu, et al., Study on aerodynamic instability and galloping response of rail overhead contact line based on wind tunnel tests, *IEEE Trans. Veh. Technol.* 72 (2023) 7211–7220, <https://doi.org/10.1109/tvt.2023.3243024>.
- [139] O.L.J.L. Chabart, Galloping of electrical lines in wind tunnel facilities, *J. Wind Eng. Ind. Aerod.* 74 (1998) 967–976, [https://doi.org/10.1016/s0167-6105\(98\)00088-9](https://doi.org/10.1016/s0167-6105(98)00088-9).
- [140] J. Wang, S. Sun, G. Hu, Y. Yang, L. Tang, P. Li, et al., Exploring the potential benefits of using metasurface for galloping energy harvesting, *Energy Convers. Manag.* 243 (2021) 114414, <https://doi.org/10.1016/j.enconman.2021.114414>.
- [141] M. Shi, A.S. Holmes, E.M. Yeatman, Piezoelectric wind velocity sensor based on the variation of galloping frequency with drag force, *Appl. Phys. Lett.* 116 (2020) 264101, <https://doi.org/10.1063/5.0012244>.
- [142] S.-D. Kwon, A T-shaped piezoelectric cantilever for fluid energy harvesting, *Appl. Phys. Lett.* 97 (2010) 164102, <https://doi.org/10.1063/1.3503609>.
- [143] F.-R. Liu, W.-M. Zhang, Z.-K. Peng, G. Meng, Fork-shaped bluff body for enhancing the performance of galloping-based wind energy harvester, *Energy* 183 (2019) 92–105, <https://doi.org/10.1016/j.energy.2019.06.044>.
- [144] G. Hu, J. Wang, L. Tang, A comb-like beam based piezoelectric system for galloping energy harvesting, *Mech. Syst. Signal Process.* 150 (2021) 107301, <https://doi.org/10.1016/j.ymssp.2020.107301>.
- [145] K. Yang, J. Wang, D. Yurchenko, A double-beam piezo-magneto-elastic wind energy harvester for improving the galloping-based energy harvesting, *Appl. Phys. Lett.* 115 (2019) 193901, <https://doi.org/10.1063/1.5126476>.
- [146] Z. Li, S. Wang, S. Zhou, Multi-solution phenomena and nonlinear characteristics of tristable galloping energy harvesters with magnetic coupling nonlinearity, *Commun. Nonlinear Sci. Numer. Simulat.* 119 (2023) 107076, <https://doi.org/10.1016/j.cnsns.2022.107076>.
- [147] C.S.C. Eloy, L. Schouveiler, Flutter of a rectangular plate, *J. Fluid Struct.* 23 (2007) 904–919, <https://doi.org/10.1016/j.jfluidstructs.2007.02.002>.
- [148] Y. Watanabe, K. Isogai, S. Suzuki, M. Sugihara, A theoretical study of paper flutter, *J. Fluid Struct.* 16 (2002) 543–560, <https://doi.org/10.1006/jfls.2001.0436>.
- [149] A. Abdelkefi, Aeroelastic energy harvesting: a review, *Int. J. Eng. Sci.* 100 (2016) 112–135.
- [150] A. Agarwal, A. Purohit, Performance evaluation of flutter-based energy harvester under different vortex flow regimes: an experimental study, *Arab. J. Sci. Eng.* 48 (2022) 3491–3501, <https://doi.org/10.1007/s13369-022-07181-x>.
- [151] G.W. Taylor, J.R. Burns, S.A. Kammann, W.B. Powers, T.R. Welsh, The energy harvesting eel: a small subsurface ocean/river power generator, *IEEE J. Ocean. Eng.* 26 (2001) 539–547, <https://doi.org/10.1109/48.972090>.
- [152] S. Orrego, K. Shoele, A. Ruas, K. Doran, B. Caggiano, R. Mittal, et al., Harvesting ambient wind energy with an inverted piezoelectric flag, *Appl. Energy* 194 (2017) 212–222, <https://doi.org/10.1016/j.apenergy.2017.03.016>.
- [153] J.M. McCarthy, S. Watkins, A. Deivasigamani, S.J. John, Fluttering energy harvesters in the wind: a review, *J. Sound Vib.* 361 (2016) 355–377, <https://doi.org/10.1016/j.jsv.2015.09.043>.
- [154] S. Pobering, Norbert Schwesinger, A novel hydropower harvesting device. International Conference on MEMS, NANO and Smart Systems, IEEE, 2004, pp. 480–485, <https://doi.org/10.1109/icmens.2004.1508997>.
- [155] F.J. Huera-Huarte, P.W. Bearman, Vortex and wake-induced vibrations of a tandem arrangement of two flexible circular cylinders with near wake interference, *J. Fluid Struct.* 27 (2011) 193–211, <https://doi.org/10.1016/j.jfluidstructs.2010.11.004>.
- [156] F.J. Huera-Huarte, Z.A. Bangash, L.M. González, Multi-mode vortex and wake-induced vibrations of a flexible cylinder in tandem arrangement, *J. Fluid Struct.* 66 (2016) 571–588, <https://doi.org/10.1016/j.jfluidstructs.2016.07.019>.
- [157] G.R.S. Assi, P.W. Bearman, N. Kitney, M.A. Tognarelli, Suppression of wake-induced vibration of tandem cylinders with free-to-rotate control plates, *J. Fluid Struct.* 26 (2010) 1045–1057, <https://doi.org/10.1016/j.jfluidstructs.2010.08.004>.
- [158] Y. Hu, B. Yang, X. Chen, X. Wang, J. Liu, Modeling and experimental study of a piezoelectric energy harvester from vortex shedding-induced vibration, *Energy Convers. Manag.* 162 (2018) 145–158, <https://doi.org/10.1016/j.enconman.2018.02.026>.
- [159] D. Zhao, J. Zhou, T. Tan, Z. Yan, W. Sun, J. Yin, et al., Hydrokinetic piezoelectric energy harvesting by wake induced vibration, *Energy* (2021) 220, <https://doi.org/10.1016/j.energy.2020.119722>.

- [160] C. Zhang, G. Hu, D. Yurchenko, P. Lin, S. Gu, D. Song, et al., Machine learning based prediction of piezoelectric energy harvesting from wake galloping, *Mech. Syst. Signal Process.* 160 (2021) 107876, <https://doi.org/10.1016/j.ymssp.2021.107876>.
- [161] X. Wu, F. Ge, Y. Hong, A review of recent studies on vortex-induced vibrations of long slender cylinders, *J. Fluid Struct.* 28 (2012) 292–308, <https://doi.org/10.1016/j.jfluidstructs.2011.11.010>.
- [162] G. Yu, J. Wen, H. Li, et al., Vibration-coupled TENGs from weak to ultra-strong induced by vortex for harvesting low-grade airflow energy, *Nano Energy.* 119 (2024) 109062, <https://doi.org/10.1016/j.nanoen.2023.109062>.
- [163] Y. Yang, L. Zheng, J. Wen, et al., A swing self-regulated triboelectric nanogenerator for high-entropy ocean breaking waves energy harvesting, *Adv. Funct. Mater.* 33 (2023) 2304366, <https://doi.org/10.1002/adfm.202304366>.
- [164] R. Li, H. Zhang, L. Wang, G. Liu, A contact-mode triboelectric nanogenerator for energy harvesting from marine pipe vibrations, *Sensors (Basel)*. 21 (2021) 1514, <https://doi.org/10.3390/s21041514>.
- [165] S. Wang, P. Xu, X. Wang, J. Zheng, X. Liu, J. Liu, et al., Underwater bionic whisker sensor based on triboelectric nanogenerator for passive vortex perception, *Nano Energy.* 97 (2022) 107210, <https://doi.org/10.2139/ssrn.4023037>.
- [166] Q. Chang, Z. Fu, S. Zhang, M. Wang, X. Pan, Experimental investigation of Reynolds number and spring stiffness effects on vortex-induced vibration driven wind energy harvesting triboelectric nanogenerator, *Nanomaterials (Basel)*. 12 (2022) 3595, <https://doi.org/10.3390/nano12203595>.
- [167] Y. Wang, T. Chen, S. Sun, X. Liu, Z. Hu, Z. Lian, et al., A humidity resistant and high performance triboelectric nanogenerator enabled by vortex-induced vibration for scavenging wind energy, *Nano Res.* 15 (2021) 3246–3253, <https://doi.org/10.1007/s12274-021-3968-9>.
- [168] L. Zhang, B. Meng, Y. Tian, X. Meng, X. Lin, Y. He, et al., Vortex-induced vibration triboelectric nanogenerator for low speed wind energy harvesting, *Nano Energy.* (2022) 95, <https://doi.org/10.1016/j.nanoen.2022.107029>.
- [169] Q. Zeng, Y. Wu, Q. Tang, W. Liu, J. Wu, Y. Zhang, et al., A high-efficient breeze energy harvester utilizing a full-packaged triboelectric nanogenerator based on flow-induced vibration, *Nano Energy.* 70 (2020) 104524, <https://doi.org/10.1016/j.nanoen.2020.104524>.
- [170] S. Zhang, Z. Jing, X. Wang, M. Zhu, X. Yu, J. Zhu, et al., Soft-bionic-fishtail structured triboelectric nanogenerator driven by flow-induced vibration for low-velocity water flow energy harvesting, *Nano Res.* 16 (2022) 466–472, <https://doi.org/10.1007/s12274-022-4715-6>.
- [171] C. Ge, J. Ma, Y. Hu, J. Li, Y. Zhang, X. He, et al., A self-powered flow velocity sensing system based on hybrid piezo-triboelectric nanogenerator, *Adv. Mater. Technol.* 8 (2022) 2201296, <https://doi.org/10.1002/admt.202201296>.
- [172] W. Wang, W. Tang, Z. Yao, A collision-free gallop-based triboelectric-piezoelectric hybrid nanogenerator, *iScience.* 25 (2022) 105374, <https://doi.org/10.1016/j.isci.2022.105374>.
- [173] Q. Wang, H.-X. Zou, L.-C. Zhao, M. Li, K.-X. Wei, L.-P. Huang, et al., A synergetic hybrid mechanism of piezoelectric and triboelectric for galloping wind energy harvesting, *Appl. Phys. Lett.* 117 (2020) 043902, <https://doi.org/10.1063/5.0014484>.
- [174] H. Kim, Q. Zhou, D. Kim, I.-K. Oh, Flow-induced snap-through triboelectric nanogenerator, *Nano Energy.* 68 (2020) 104379, <https://doi.org/10.1016/j.nanoen.2019.104379>.
- [175] H. Phan, D.-M. Shin, S. Heon Jeon, T. Young Kang, P. Han, G. Han Kim, et al., Aerodynamic and aeroelastic flutters driven triboelectric nanogenerators for harvesting broadband airflow energy, *Nano Energy.* 33 (2017) 476–484, <https://doi.org/10.1016/j.nanoen.2017.02.005>.
- [176] Y. Wang, E. Yang, T. Chen, J. Wang, Z. Hu, J. Mi, et al., A novel humidity resisting and wind direction adapting flag-type triboelectric nanogenerator for wind energy harvesting and speed sensing, *Nano Energy.* 78 (2020) 105279, <https://doi.org/10.1016/j.nanoen.2020.105279>.
- [177] Y. Wang, X. Liu, Y. Wang, et al., Flexible seaweed-like triboelectric nanogenerator as a wave energy harvester powering marine internet of things, *ACS Nano.* 15 (2021) 15700–15709, <https://doi.org/10.1021/acsnano.1c05127.s004>.
- [178] A. Ahmed, I. Hassan, P. Song, et al., Self-adaptive bioinspired hummingbird-wing stimulated triboelectric nanogenerators, *Sci. Rep.* 7 (2017) 17143, <https://doi.org/10.1038/s41598-017-17453-4>.
- [179] S. Yuan, Q. Zeng, D. Tan, Y. Luo, X. Zhang, H. Guo, et al., Scavenging breeze wind energy (1–8.1 ms⁻¹) by minimalist triboelectric nanogenerator based on the wake galloping phenomenon, *Nano Energy.* 100 (2022) 107465, <https://doi.org/10.1016/j.nanoen.2022.107465>.
- [180] Y. Wang, X. Liu, T. Chen, H. Wang, C. Zhu, H. Yu, et al., An underwater flag-like triboelectric nanogenerator for harvesting ocean current energy under extremely low velocity condition, *Nano Energy.* 90 (2021) 106503, <https://doi.org/10.1016/j.nanoen.2021.106503>.
- [181] J. Wang, S. Zhou, Z. Zhang, D. Yurchenko, High-performance piezoelectric wind energy harvester with Y-shaped attachments, *Energy Convers. Manag.* 181 (2019) 645–652, <https://doi.org/10.1016/j.enconman.2018.12.034>.
- [182] F.-R. Liu, W.-M. Zhang, L.-C. Zhao, H.-X. Zou, T. Tan, Z.-K. Peng, et al., Performance enhancement of wind energy harvester utilizing wake flow induced by double upstream flat-plates, *Appl. Energy* 257 (2020) 114034, <https://doi.org/10.1016/j.apenergy.2019.114034>.
- [183] Z. Zhao, X. Pu, C. Du, L. Li, C. Jiang, W. Hu, et al., Freestanding flag-type triboelectric nanogenerator for harvesting high-altitude wind energy from arbitrary directions, *ACS Nano.* 10 (2016) 1780–1787, <https://doi.org/10.1021/acsnano.5b07157.s001>.
- [184] I.-W. Tcho, W.-G. Kim, J.-K. Kim, D.-W. Kim, S.-Y. Yun, J.-H. Son, et al., A flutter-driven triboelectric nanogenerator for harvesting energy of gentle breezes with a rear-fixed fluttering film, *Nano Energy.* 98 (2022) 107197, <https://doi.org/10.1016/j.nanoen.2022.107197>.